

ADVANCES AND REMAINING CHALLENGES FOR GEOSYNTHETICS IN GEOENVIRONMENTAL ENGINEERING APPLICATIONS*

R. Kerry Rowe**

ABSTRACT – Nine issues of importance to the use of geomembranes (GMs) and geosynthetic clay liners (GCLs) as part of composite liners in geoenvironmental applications are examined. These issues include the effect of: GCL-leachate compatibility on hydraulic conductivity; freeze-thaw on GCL performance; internal erosion on GCL hydraulic conductivity; temperature on advection and diffusion as well as desiccation of GCLs and compacted clay liners (CCLs); the choice of protection layer on the strains developed in GMs; wrinkles on strains developed in GMs and the thinning of GCLs; holes in GMs on leakage through composite liners; wrinkles in GMs on leakage through composite liners; diffusion through GCLs and GMs; and temperature and leachate exposure on the service life of GMs. It is suggested that GCLs and GMs can play a very beneficial role in providing environmental protection. However, like all engineering materials they must be used appropriately and consideration should be given to factors such as those addressed in this paper. There is a need for site specific design, strict adherence to construction specification, and appropriate protection of the geosynthetics after construction. In particular, given the diversity of available GCLs and their different engineering characteristics, GCLs should be selected based on the required engineering properties, not just price.

KEY WORDS – geomembranes, geosynthetic clay liners, composite liners, geoenvironmental, hydraulic conductivity, clay-leachate interaction, freeze-thaw, internal erosion, leakage, diffusion, ageing.

1 – INTRODUCTION

In recent years there have been many advances in the understanding of issues related to the use of geosynthetics such as geosynthetic clay liners (GCLs) and geomembranes (GM) as contaminant barriers. As a consequence there has also been a significant increase in geoenvironmental applications. These applications range from the more traditional use of GCLs and GMs as composite base liners or as part of capping systems for landfills (*e.g.* Rowe *et al.*, 2004b), as liners for contaminated fluids (*e.g.* leachate lagoons, Rowe *et al.*, 2003), as barriers to contain past spills of hydrocarbons (*e.g.* Bathurst *et al.*, 2006), as secondary containment around fuel tanks to prevent possible future contamination in the event of a tank rupture or equipment malfunction, as containment for fluids in heap leach pads (Thiel & Smith, 2004), and as covers and liners for mine waste (*e.g.* Lange *et al.*, 2005).

The objective of this paper is to highlight some of the recent advances in geosynthetic engineering, illustrate some of the important considerations related to design and construction using geosynthetics, and flag some of the remaining challenges related to the use of geosynthetics in geoenvironmental applications. Attention will be primarily focused on data and findings published since 2000. Readers requiring an introduction to the use of geosynthetics in barrier applications are referred to Rowe *et al.* (2004b).

* Reprodução do trabalho publicado na revista Soils & Rocks - International Journal of Geotechnical and Geoenvironmental Engineering, vol. 30, n° 1, 3-30, 2007.

** R. Kerry Rowe, Ph.D., Professor and Vice-President (Research), GeoEngineering Centre at Queen's-RMC, Department of Civil Engineering, Queen's University, Kingston, ON, K7L 3N6, Canada. e-mail: kerry@civil.queensu.ca.

This paper will address nine issues of importance to the use of geosynthetics in geoenvironmental applications: (1) GCL-leachate compatibility; (2) the effect of freezethaw on GCL performance; (3) internal erosion of GCLs; (4) temperature; (5) protection of composite liners; (6) wrinkles in GMs; (7) holes in GMs and the consequent leakage through composite liners; (8) diffusion through GCLs and GMs; and (9) service life of GMs. This paper is intended to complement two other extensive examinations of the use of geosynthetics in landfills (Rowe, 1998; Rowe, 2005) and incorporates, but expands on, material presented by Rowe (2006). With respect to issue 1, this paper updates the review reported by Rowe (1998) however there is much valuable information in the 1998 paper which is not repeated here. Issues 2 and 3 are not addressed in either of these earlier papers. Issues 4-9 are discussed in both of these previous papers. This paper will only discuss issues 4 and 9 to the extent necessary to provide context of the overall thrust of designing safe long-term containment and, where appropriate, broadening their applicability to applications beyond landfills or providing new information. The reader is referred to Rowe (2005) for a more in-depth discussion of these issues. In contrast this paper will provide much more detail with respect to issues 3, 5, 6, 7 and 8 than was provided in either previous paper.

2 – GCL-LEACHATE COMPATIBILITY

2.1 – Municipal solid waste (MSW) leachate

Many researchers (*e.g.* Schubert, 1987; Shan & Daniel, 1991; Daniel *et al.*, 1993; Dobras & Elzea, 1993; Ruhl & Daniel, 1997; Petrov *et al.*, 1997; Petrov & Rowe, 1997; Kodikara *et al.*, 2002; Ashmawy *et al.*, 2002; Kolstad *et al.*, 2004; Katsumi & Fukagawa, 2005; Lee & Shackelford, 2005; Guyonnet *et al.*, 2005; Jo *et al.*, 2005, 2006) have discussed the issue of GCL-leachate compatibility and its effect on the hydraulic conductivity of GCLs. The hydraulic conductivity of a GCL has been shown to be highly dependent on: the hydrating conditions, the applied effective stress during permeation, the method of GCL manufacture, and the mass of bentonite in the GCL (Rowe, 1998). For example, Petrov & Rowe (1997) showed that if there is a low applied stress at the time of permeation, there can be an order of magnitude increase in hydraulic conductivity to about 6×10^{-10} m/s as the permeant was changed from water to MSW leachate (Table 1). The effect was far less significant at higher confining stress and the hydraulic conductivity to MSWleachate was still very low at 3×10^{-11} m/s. It has been shown that consolidation during permeation can greatly mitigate the effects of clay-leachate interaction on hydraulic conductivity.

Table 1 – Effect of applied stress on hydraulic conductivity with respect to water and MSW leachate (after Petrov & Rowe,1997).

Hydration stress (kPa)	Hydrated thickness (mm)	Hydraulic conductivity to water (m/s)	Hydraulic conductivity to MSW Leachate (m/s)
3	12.3	6×10^{-11}	55×10^{-11}
115	6	0.75×10^{-11}	3×10^{-11}

The hydraulic conductivity (k) of a GCL for a given permeant can be directly related to the bulk void ratio of the GCL (e_b) (Petrov *et al.*, 1997). For example, for a particular GCL and MSWleachate it can be shown that there is a relatively straightforward relationship between k and e_b , viz:

$$-11.4 + 0.42e_b < \log_{10} k \text{ (m/s)} < -11.2 + 0.42e_b \quad (1)$$

Relationships such as this will be both product and permeant dependent but can be established for any given design situation.

Rowe (1998) demonstrated that when dealing with composite liners, the ability of the GCL to minimize leakage through holes in a GM is not especially sensitive to the hydraulic conductivity of the GCL but, rather, is much more dependent on the interface transmissivity between the GM and the GCL. This helps explain the low leakage reported for composite liners with a GCL as discussed later. Nevertheless consideration should be given to the potential increase in k due to interaction with the leachate and the expected values should be used in the design leakage calculations. Interaction is expected to be greatest for a GCL used in applications where there is low applied stress and high concentrations of salts (especially those with divalent cations). An example of a potentially problematic application would be the use of a GCL as part of a composite liner for a lagoon to contain brines. Applications such as this will require special attention and possibly a GCL with an amended bentonite (rather than the typical sodium bentonite) selected based on clay-permeant compatibility considerations.

2.2 – Mine waste waters

The control metal and metalloid contamination derived from waste rock and mine tailings is a major challenge for the mining industry. Past research has focused on covers which reduce acid production by limiting infiltration and oxygen. While there is certainly a need to deal with acid drainage, recent research has suggested that potentially toxic elements (*e.g.* arsenic, selenium and, sometimes, nickel and zinc) can be mobile under neutral-pH conditions. Also reductive dissolution of As-bearing minerals can lead to the release of As (Stichbury *et al.*, 2000). This increases interest in segregating the most hazardous wastes for separate disposal in a fully lined containment facility. GCLs have a potential role to play in containing these contaminants.

The attenuation of single metal and multi-metal permeants by sodium bentonite and similar clay combinations have been examined by a number of investigators (*e.g.* Brain, 2000; Li & Li, 2001; Cooper *et al.*, 2002; Abollino *et al.*, 2003). The primary mechanisms controlling metal mobility in sodium bentonite are (Abollino *et al.*, 2003): (i) cation exchange within the clay lattice structure; and (ii) cation attraction to broken bonds at the edges of the clay mineral. Other mechanisms include (iii) limited anion exchange (30 meq/100 g) where the anions typically attach to the clay structure by substitution of hydroxides at the edges of gibbsite sheets (McKelvey, 1997), and (iv) attenuation of metals by precipitation (Yong, 2001). It is well known that soil pH, redox, and soil porewater composition can have a significant impact on metal mobility (Yong, 2001).

Lange *et al.* (2004, 2005) studied the potential for metal (Al, Fe, Mn, Ni, Pb, Cd, Cu, Zn) migration through GCLs from an acid rock drainage (ARD) solution (pH 3.9). Mn was found to experience the least attenuation and its migration was similarly to Cl. The ARD effluent remained neutral for about 11 pore volumes of permeation during which time Al, Fe and Cu were highly retarded and retained within the clay. Ni, Zn, and Cd were moderately attenuated. The Fe, Zn, Mn, As, Pb and Al were primarily attenuated in the upper portion of the GCL. There was evidence to suggest that Fe and Mn were predominantly attenuated by precipitation of Fe-Mn oxyhydroxides. Ni and Cu were fairly uniformly attenuated throughout the thickness of the GCL.

As the buffering capacity of the bentonite was depleted and eventually exhausted, the pH decreased until it eventually reached the influent value of 3.9 after 35 PVs of permeation. The shift in pH resulted in some metals being remobilized from the bentonite back into solution. Thus for ARD solutions there is considerable potential to retard metals but this potential is limited by the

buffering capacity of the bentonite. In a design situation, this can be related to the mass per unit area of bentonite in the GCL and the expected flow through the GCL. The hydraulic conductivity of the GCLs permeated with ARD increased from 2.8×10^{-12} m/s to 3.7×10^{-11} m/s after 35 pore volumes of permeation.

Lange *et al.* (2007) also examined the interaction between a GCL and gold mine leachate (GML). The GML had much higher concentration of Ca^{2+} and Mg^{2+} than the ARD (Table 2) but despite this the concentration of these cations in the effluent from the GCLs permeated with GML was much lower than was observed in the ARD tests. This can be attributed to cation exchange resulting from the high metal loading together with displacement by H^+ ions.

Table 2 – Initial concentrations of permeant liquids examined by Lange *et al.* (2005).

Parameter*	Gold mine leachate(GML)	Acid rock drainage (ARD) leachate
Calcium (Ca^{2+})	110.1	0.7
Sodium (Na^+)	964.0	457.7
Sulphate (SO_4^{2-})	2447.0	2932
Potassium (K^+)	8.0	779.9
Magnesium (Mg^{2+})	83.5	0.15
Strontium (Sr^{2+})	2.2	n/a
Manganese (Mn^{2+})	2.1	26.59
Aluminium (Al^{3+})	3.56	88.73
Iron (Fe^{2+})	0.41	214.4
Copper (Cu^{2+})	n/a	19.7
Chloride (Cl^-)	268.0	69
Cadmium (Cd^{2+})	2.1	4.9
Nickel (Ni^{2+})	n/a	20.2
Arsenic (As^{5+})	4.0	4.2
Zinc(Zn^{2+})	n/a	107.2
Lead (Pb^{2+})	n/a	13.9
pH	6.85	3.7

All units in mg/L, with exception of pH; *the valence indicated refers to how the ion was initially introduced.

Although both the ARD and GML had high concentrations of sulphate, there was much greater retention of the sulphate by the GCL in the GML tests than in the ARD tests, with much of the sulphate being precipitated in the upper portion of the GCL as gypsum for the GML tests but not for the ARD tests. The significant attenuation of Cd in the GML was presumed to be largely associated with precipitation of gypsum because Huang *et al.* (1999) had demonstrated that Cd can adsorb to gypsum during its crystal growth. There was also more attenuation of arsenic for the ARD samples than the GML samples. The attenuation of arsenate in the GML was also partly attributed to gypsum precipitation with As oxyanions substituting for SO_4^{2-} in the gypsum structure.

2.3 – Hydrocarbons

Several investigators have examined the effect of organic permeants on the hydraulic conductivity of GCLs. This has included consideration of neat and diluted ethanol (Petrov *et al.*, 1997),

gasoline (Shan & Lai, 2002) and Jet A-1 (Rowe *et al.*, 2004a). Because of the hydrophobic nature of many organic contaminants there can be a threshold pressure below which there is no permeation of the hydrocarbon through a water saturated GCL. For example, Shan & Lai (2002) reported no flow of gasoline through a GCL under a hydraulic gradient of 150 over a test period of 3 weeks. Likewise, Rowe *et al.* (2007a) found that there was no flow of Jet A-1 through a hydrated GCL until the pressure difference between the two sides of the GCL exceeded 27 kPa. These tests were conducted with a flexible wall permeameter. Rigid wall permeameters are also commonly used to obtain k and Rowe *et al.* (2005a) showed that in these tests, the k of GCLs permeated with Jet A-1 increased with increasing hydraulic gradient. This is thought to be because the higher pressures associated with higher gradients overcome interfacial tensions in the smaller pores thereby opening up more flow paths than were available at lower gradients. As a consequence, the values deduced from rigid wall permeameter tests at high gradients may considerably overestimate the k that would actually be mobilized in field applications.

It can be concluded from the foregoing that hydrated GCLs can be an excellent hydraulic barrier to hydrophobic hydrocarbons like Jet A-1 in the many practical applications where the hydrocarbon head does not exceed the threshold value.

3 – FREEZE-THAW

While there are many applications where a GCL will not be subjected to freezing, there are also many parts of the world where GCLs will be subjected to freeze-thaw cycles. Hewitt & Daniel (1997), Kraus *et al.* (1997), Rowe *et al.* (2007a) and Podgorney & Bennett (2006) performed tests on GCLs subjected to 3, 20, 100 and 150 freeze-thaw cycles respectively and found that there was no significant change in k of a GCL with respect to water due to these freeze-thaw cycles. While this is very positive, it should be noted that these tests did not examine the effect of potential interaction of the GCL with the pore water in adjacent soils. If these soils have pore fluid with divalent cations (*e.g.* Ca^{2+} or Mg^{2+}) then cation exchange of these cations for Na^+ on the sodium bentonite in the GCL can result in an increase in k of the GCL both in the laboratory (Shackelford *et al.* 2000; Egloffstein 2001; Jo *et al.* 2001, 2004, 2005) and field (James *et al.* 1997; Melchior 1997, 2002; Egloffstein 2001). This, combined with a reduction in swell index due to cation exchange and freeze-thaw, has the potential to give rise to an increase in k of the GCL with time unless the GCL is subjected to sufficient confining stress to prevent shrinkage and crack formation under the combined influence of double layer contraction and ice lensing. Egloffstein (2001, 2002) has suggested that a 0.75-1.0 m thick soil cover is sufficient to protect GCLs from significant increase in hydraulic conductivity. However more research is required to assess the potential effect of relatively low stress and freeze-thaw cycles on the long-term performance of GCLs used in covers and similar near surface applications to confirm when Egloffstein's suggestion is generally applicable.

The effects of freeze-thaw on k of GCLs with respect to hydrocarbons has, until recently, received little attention. This is important for cases like those described by Bathurst *et al.* (2006) where a composite liner was used to contain a hydrocarbon spill at a former DEW-Line site on Brevoort Island in the Canadian Arctic until there can be future remediation. In this case shallow permafrost provides a natural barrier to prevent significant downward migration of hydrocarbons. However an engineered barrier was required to prevent lateral spreading of the hydrocarbon plume. The geosynthetic composite barrier composed of a fluorinated high density polyethylene (f-HDPE) and GCL was installed to cut off flow of hydrocarbons to the sea in the active zone above the

permafrost in 2001. Another GM was used to cover the surface area between the source of the plume and the barrier to minimize infiltration of rainwater or runoff into the contaminated zone. The barrier is unfrozen in the summer months but frozen for most of the remainder of the year. Thus the question arises as to how effective the GCL will be as a barrier to hydrocarbons after being subjected to freeze-thaw cycles.

Rowe *et al.* (2004a, 2006, 2007a) performed freeze and thaw tests using flexible wall (FWP) and rigid wall (RWP) permeameters. The GCL samples were hydrated for five days under low confining pressure (15 ± 3 kPa), subjected to up to 100 freeze and thaw cycles, and then first permeated with de-aired water followed by Jet A-1. Tests were also conducted on samples recovered from the field after 1 and 3 years natural exposure to the groundwater and freeze-thaw in the arctic.

Rowe *et al.* (2006) used RWP to permeate GCLs with Jet A-1 until equilibrium was reached. The mean equilibrium k was about 8.0×10^{-11} and 14.5×10^{-11} m/s for 5 and 12 freeze-thaw cycles respectively (*i.e.* about 4.0 and 5.6 times greater than the initial value with respect to water). Thus the combination of high gradients and many pore volumes of permeation increased both the intrinsic permeability and k . This was due to an increase in the pore size with SEM images showing that the bentonite pore size for GCLs subjected to up to 12 freeze-thaw cycles was 2-3 times larger than that of the bentonite in the virgin GCL. Application of Olsen's (1961) cluster model suggested that the double layer contracted by 20-40% after permeating with Jet A-1 while the free-space expanded 1.2-2.5 times that before Jet A-1 permeation.

Tests performed using flexible wall permeameters (Rowe *et al.*, 2007a) found that the threshold pressure of Jet A-1 for hydrated GCLs with no freeze-thaw cycles was between about 27 to 55 kPa. The range of threshold pressure for GCLs exhumed from the field after 3 years and those subjected to up-to 50 freeze-thaw cycles in the laboratory was 13.8-20.7 kPa (*e.g.* see Fig. 1). This reduced to between 0 and 13.8 kPa after 100 freeze-thaw cycles. Thus, freeze-thaw did reduce the threshold pressure and this is attributed to an increase in the size of macro pores in the bentonite following repeated freeze-thaw cycles.

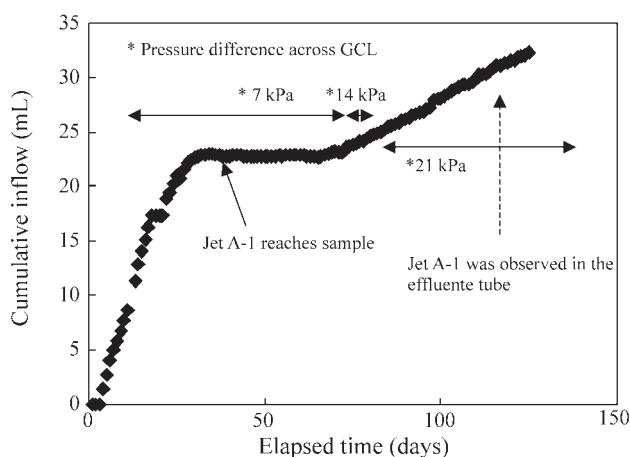


Fig. 1 – Variation in cumulative inflow volume through the GCL with time for a GCL subjected to 12 freeze and thaw cycles and permeated with water and Jet A-1 in flexible wall permeameter test (modified from Rowe *et al.*, 2005c).

The k (with respect to Jet A-1) of the hydrated GCL recovered from the field after 3 years was less than 3×10^{-12} m/s. The k after up to 50 freeze-thaw cycles in the laboratory was less than 3×10^{-11} m/s at a gradient just above that required to initiate flow. There was some increase in k with 100 freeze-thaw cycles with a maximum value of about 1×10^{-10} m/s. Thus both the laboratory and field evidence suggest that the GCL will provide an effective barrier to hydrocarbons for many years and up to 100 freeze-thaw cycles for the conditions present at Brevoort Island.

4 – INTERNAL EROSION

GCLs are commonly used in applications where there may be several to many meters of fluid over the GCL (*e.g.* ponds, lagoons, and landfills when a leachate mound builds up). Since GCLs are relatively thin, these applications can give rise to high gradients and the potential for internal erosion. This is particularly true when the GCL is placed over gravel or a geonet (*e.g.* in a double lined landfill). Giroud & Soderman (2000) conducted an analysis of the implications of bentonite loss from GCLs used above geonet drainage layers and concluded that a bentonite loss in excess of about 100 g/m^2 (*i.e.* about 2.5% of the initial bentonite mass) would impact on the GCL k and that for these applications the impact on drainage was more severe than the impact on the permeability of the GCL. Based on this analysis, they concluded that 10 g/m^2 (*i.e.* about 0.25%) could be used as a limit for impact on the drainage layer. Failures have occurred due to internal erosion. For example, Stam (2000) reported a field case where a GCL was used to line a lake. Following observations of excessive leakage, an investigation found “patchy” bentonite piping from the core of the GCL through the lightweight nonwoven geotextile resting on the coarse sand subgrade. While researchers have shown that damaged GCLs can self-heal with only a slight increase in k this self-healing process can be compromised and significant bentonite loss can occur if the damaged GCLs are placed on a coarse subgrade with large pore openings (Mazzieri & Pasqualini, 2000).

Rowe & Orsini (2003) studied the performance of five different GCLs (Table 3) resting on a geonet (opening size of 0.8 cm and a diagonal span of 1.2 cm), 6 mm uniform gravel ($d_{85} \approx 7 \text{ mm}$, $d_{50} \approx 6 \text{ mm}$, $d_{15} \approx 3.6 \text{ mm}$ and $d_{10} \approx 3 \text{ mm}$), and a well graded sand ($d_{85} \approx 1.1 \text{ mm}$, $d_{50} \approx 0.17 \text{ mm}$, $d_{15} \approx 0.043 \text{ mm}$ and $d_{10} \approx 0.03 \text{ mm}$). Their findings are summarized in the following paragraphs.

When placed on the geonet, four of the five GCLs tested (BWD, NWD, WD, SNWD; see Table 3) experienced internal erosion (bentonite loss) and an increase in hydraulic conductivity by at least one order of magnitude for heads ranging from 8 m to 45 m. In contrast the BSNWD scrim-reinforced GCL with a total carrier geotextile mass per unit area of 350 g/m^2 did not exhibit any sign of internal erosion (at heads of up to 55 m).

When placed directly over the 6 mm gravel GCLs with a single woven geotextile (BWD, WD, and NWD with the woven down) in contact with the geonet and the NWD (with the light nonwoven geotextile in contact with the geonet) all experienced internal erosion. In these cases the hydraulic conductivity increased by at least one order of magnitude for water heads ranging from ~8 m to ~90 m. In contrast, the scrim-reinforced GCLs (SNWD, BSNWD) did not experience any detrimental effects at hydraulic heads of 40-60 m for the conditions examined.

All of the GCLs tested performed well when placed over the well graded sand subgrade. For these cases even heads in the range 50-80 m did not cause any significant bentonite loss and there was no evidence of internal erosion for GCLs placed over this sand subgrade.

As the loss of bentonite increased, so too did the k . However failures, characterized by a significant increase in k of the specimen, could initially be quite localized and in some cases failure

Table 3 – GCLs used in internal erosion tests (after Rowe & Orsini, 2003).

GCL	Product descriptor	Upper geotextile ¹	Core sodium bentonite	Lower geotextile ¹	Total mass/unit area (g/m ²)	Bentonite moisture content (%)
BWD ²	BFG5000	Bentonite filled (800 g/m ²) nonwoven 300 g/m ²	Powder 4200 g/m ²	Slit film woven 200 g/m ²	5500	< 15
WD ²	NS	Staple fibre nonwoven 200 g/m ²	Granular 4340 g/m ²	Slit film woven 105 g/m ²	4645	< 12
NWD ³	ST	Nonwoven 220 g/m ²	Granular 4800 g/m ²	Slit film woven 100 g/m ²	5100	22
SNWD ²	NW	Staple fibre nonwoven 200 g/m ²	Granular 4340 g/m ²	Slit film woven, nonwoven composite 305 g/m ²	4845	< 12
BSNWD ²	B4000	Nonwoven 300 g/m ²	Powder 4700 g/m ²	Slit film woven (100 g/m ²), nonwoven (250 g/m ²) composite	5350	< 15

¹Polypropylene; ²Bentofix, thermally-treated and needle-punched; ³Bentomat, needle-punched.

was associated with relatively little bentonite loss (as little as 1%). This suggests that the limit proposed by Giroud & Soderman (2000) of about 10 g/m² (about 0.25%) may be appropriate as a conservative limit for both hydraulic and drainage considerations. Rowe & Orsini (2003) concluded that designs involving GCLs over a gravel or geonet subgrade need to be carefully examined since internal erosion at water heads as low as 8 m caused an increase in the k by one to two orders of magnitude. The gravel used in their tests meet the subgrade criteria of ASTM D6102, and thus it appears that GCL installations meeting this standard could experience internal erosion and fail under water heads encountered in reservoirs, lagoons or landfills where leachate mounding occurs.

Rowe & Orsini's work showed that the choice of GCL carrier geotextile could significantly affect GCL performance. A GCL with a woven geotextile down (*i.e.* in contact with the 6 mm gravel and geonet) did not perform as well as the other GCLs. GCLs with a nonwoven down performed better for the gravel subgrade, but neither was acceptable for a GCL placed over the geonet. The heavy scrim-reinforced GCLs performed best with BSNWD working well for all cases examined.

For the specific well graded sand subgrade tested, all GCLs performed well. This highlights the need to carefully consider the choice of GCL in the context of the expected gradient and subgrade conditions.

5 – TEMPERATURE

5.1 – Temperature at the base of a landfill

Heat generated by biodegradation of waste or the heat of hydration of incinerated residues (ash) are known to increase the temperature at the base of a landfill. The temperature typically has a maximum value in the main body of the waste and decreases towards the boundaries defined by

the surface and the underlying liner (Fig. 2). The rate of increase in temperature with time both in the waste and at the liner may vary depending on the waste management practice that is adopted. For example, Fig. 3 shows temperatures ranging from 24-38 °C below 4-6 year old waste at the Altwarmbüchen Landfill in Germany where waste was placed at a rate of 10-20 m/a but only 14-20 °C after a similar period at the Venneberg Landfill where waste was placed at 2 m/a. The availability of moisture can also have a profound effect on temperature as illustrated by Koerner & Koerner (2006) who monitored the temperature on the GM liner beneath 50 m of waste at two landfill cells north of Philadelphia, USA (mean annual temperature 12.6 °C). The cells had a similar low permeability geosynthetic cover but in one case (“dry cell” in Fig. 4) there was no additional moisture added while in the other case (“wet cell” in Fig. 4) there was moisture augmentation at a rate of approximately 500 m³ per month. For the dry cell, the average liner temperature has increased to about 32 °C after 10 years. In contrast for the wet cell the temperature increased rapidly to between 41-46 °C.

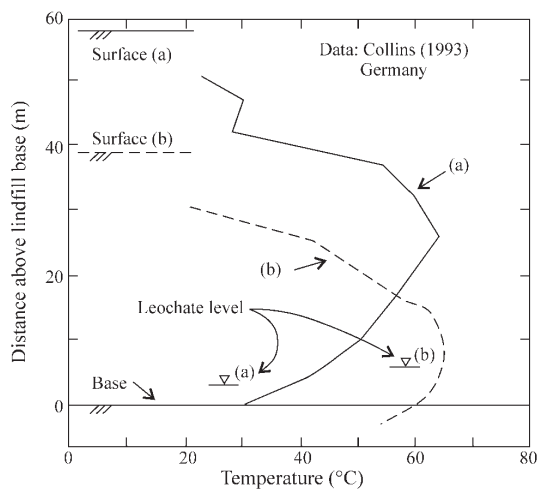


Fig. 2 – Temperature variation with depth at two locations, (a) and (b), in an old landfill (1936-1980) in Hannover Germany; waste circa 1938 at bottom (after Rowe, 1998).

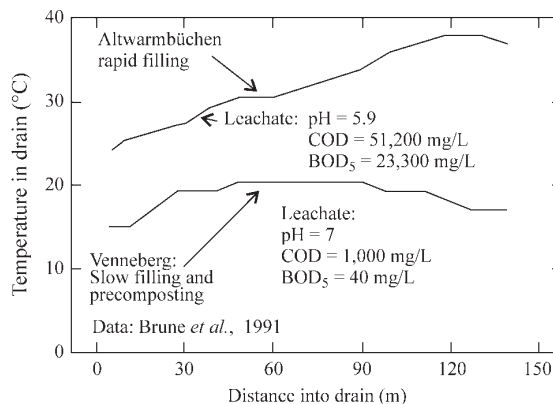


Fig. 3 – Temperature in drains at two German landfills approximately 4 years after last waste placed above the drains (modified from Brune et al., 1991).

At the Keele Valley Landfill (KVL) in Canada the temperatures above the liner appear to be leveling off in the 30-40 °C range (“Canada” in Fig. 4). Even higher temperatures have been reported in older landfills without a leachate collection system. For example, at the Tokyo Port Landfill in Japan the temperatures at the base (“Japan” in Fig. 4) were up to 50 °C 7-10 years after the beginning of landfilling and have reduced to 37-41 °C after 20 years (Yoshida & Rowe, 2003). High temperature is not restricted to MSW landfills. At the Ingolstadt landfill in Germany (“Germany” in Fig. 4), hydration of 9 m of MSW incinerator bottom ash produced a liner temperature of 463 °C 17 months after the start of landfilling.

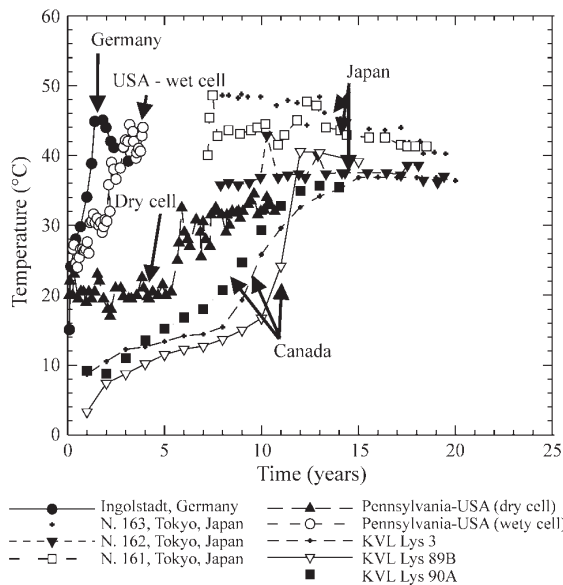


Fig. 4 – Some observed temperatures at the base of landfills (US data: Koerner & Koerner, 2006; Canadian data: Rowe, 2005; Japanese data: Yoshida & Rowe, 2003; German data: Klein *et al.* 2001).

Temperature influences both k and diffusion coefficient. Table 4 gives the ratio of both the diffusion coefficient and k at different temperatures to that at 10 °C (typical groundwater temperature in many parts of the world). Diffusive and advective transport is, respectively, 100% and 80% higher at 35 °C than at 10 °C (Table 4). Temperature also has a significant impact on service lives of GMs and clay liners as will be discussed later.

Table 4 – Effect of temperature on diffusion coefficient, DT , and hydraulic conductivity, kT , in a liner at temperature, T , relative to values at 10 °C (after Rowe, 1998).

Temperature (°C)	D_T/D_{10}	k_T/k_{10}
10	1.0	1.0
20	1.4	1.3
25	1.6	1.5
35	2.0	1.8
50	2.7	2.4
65	3.5	2.9

The discussion above deals with the temperature at the top of the primary liner. The temperature at the top of the secondary liner will depend on the thermal insulation provided by the material between the primary and secondary GM liner. In the case of double composite liner systems involving just a GM and GCL as the primary liner, unpublished measurements indicate that the temperature of the secondary GM may only be 3 °C or less below that of the primary GM (Legge, pers. comm.). This is consistent with theoretical modelling conducted by Rowe & Hoor (2007) which suggested only about a 1 °C difference assuming no cooling is induced by the leak detection layer. If there is a compacted clay liner (CCL) or foundation layer as part of the primary liner, then the added thermal resistance will lead to a reduction in the increase in temperature on the secondary GM that will depend primarily on the thickness of the clay liner/foundation layer. As shown in Fig. 5, for a steady state 40 °C increase in temperature relative to ground water temperature on the primary GM (*i.e.* a primary GM temperature of 50 °C if groundwater temperature is 10 °C), there would be a 30 °C increase on the secondary liner for a 0.75 m thick CCL. The calculated increase in temperature in secondary GM for CCL thicknesses of 0.5, 0.75 and 1 m was 33, 30 and 28 °C respectively. For a 20 °C increase at the primary GM (*i.e.* a primary GM temperature of 30 °C if groundwater temperature is 10 °C), the temperature increase at the secondary GM below a 0.75 m thick CCL and 0.3 m leak detection system would be 15 °C. This needs to be considered when assessing the service life of the secondary GM and the potential for desiccation of the secondary clay liner.

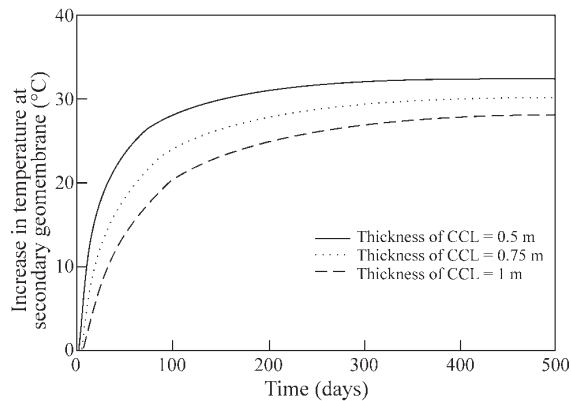


Fig. 5 – Effect of primary liner thickness on temperature of secondary geomembrane assuming a 40 °C increase on the primary liner (after Rowe & Hoor, 2007).

5.2 – Effect of temperature on GCLs and CCLs

Both GCLs and CCLs are susceptible to shrinkage and desiccation cracking, particularly when below a GMin a composite liner. Geomembrane temperature is very sensitive to solar radiation and can reach 80 °C (Felon *et al.*, 1992). An increase in GM temperature can cause evaporation of water from the underlying GCL into any air space between the GCL and the GM and subsequent movement of this water down-slope upon cooling of the GM. The temperature gradient beneath the GM can also cause migration of moisture from the GCL into the subsoil. Field examples involving desiccation of CCLs and shrinkage of GCLs due to temperature increase induced by solar radiation have been reported by Corser *et al.* (1992), Basnett & Bruner (1993), and Thiel & Richardson (2005). Laboratory studies also suggest that some GCLs are more susceptible to shrinkage than others (Thiel *et al.*, 2006).

Rowe (2005) has provided a recent review of research relating to the desiccation of CCLs and GCLs due to thermal gradients generated by the waste and the reader is referred to that source for details. Based on the numerical studies conducted by Heibrock (1997) and Southen (2005), and the experimental data published by Southen & Rowe (2004, 2005), Rowe (2005) reached a number of tentative conclusions as described below.

The potential desiccation of composite liner systems (both GM/GCL and GM/CCL) is controlled by the temperature gradient (and hence the temperature at the top of the liner). As discussed earlier, this may be a function of landfill operation and the likely temperatures to be experienced at the liner need to be considered in landfill design. For single composite liners involving a GCL, it was suggested that:

(a) The unsaturated soil characteristics and initial water content of the foundation layer beneath the GCL greatly influences the potential for desiccation.

(b) The greater the overburden stress at the time of GCL hydration, the lower is the risk of desiccation. Thus both the potential for short term (*e.g.*, solar induced) and long term (waste temperature induced) desiccation can be minimized by placing the waste over the composite liner as quickly as possible after the liner construction. This finding has significant implications for the manner in which many landfills are developed.

(c) Increasing distance to the underlying watertable increased the risk of desiccation for aquifer depths up to about 5 m below the GCL, but relatively little change was predicted for increased depths beyond 5m due to the offsetting effects of reduced water content and temperature gradient.

For single composite liners involving a CCL, it was suggested that:

(a) The unsaturated soil characteristics of the liner had a significant effect on the distribution of moisture and stress.

(b) The effect of overburden stress was not as significant as for a GCL, although it did still reduce the risk of desiccation.

There is a need for more research into the potential for long-term desiccation of clay liners making up part of a composite liner, especially with respect to the paucity of relevant soil parameters. Current research suggests that there is real potential for desiccation but also suggests that this can be mitigated by appropriate design and construction.

6 – PROTECTION OF COMPOSITE LINERS

Geomembrane protection layers most commonly used in North America involve a relatively light needlepunched nonwoven geotextile. This arises, in part, because a geotextile with a mass per unit area as low as 270 g/m² has been reported (Reddy *et al.*, 1996) to “completely protect the GM from construction loading”. Wilson-Fahmy *et al.* (1996), Narejo *et al.* (1996), and Koerner *et al.* (1996) demonstrated a linear increase in protection resistance with increasing thickness (mass per unit area) of the protection layer and proposed a methodology for selection of geotextile protection layers that will provide short-term protection against puncture under the loads applied by the overlying waste. Badu-Tweneboah *et al.* (1998) proposed a test methodology to assessing the suitability of a protection layer. This approach involves three steps. Firstly, do a full scale test with the actual materials that are being considered for the project (gravel leachate collection layer, protection layer, GM, and subgrade, as appropriate) and subject the system to loads as close as possible to the anticipated loads (construction loads, in-service loads). Secondly, take the GM from

the system and conduct a large diameter (0.5m or more) burst test (hydrostatic test). If inflation is impossible, this means that the GM specimen has a hole (which may not have been visible) and the GM specimen fails the test. If inflation is possible, inflate until the GM fails. If failure occurs at the apex of the dome, the point of maximum stress, then the GM specimen passes the test. If failure of the GM occurs at a location other than the apex of the dome, then the GM has been weakened in the field test and consequently fails the test. Thirdly, if the GM failed, redo the first two steps with different protection layers until a satisfactory design is achieved.

Tognon *et al.* (2000) performed large-scale physical testing of a number of different protection layers and showed that the protection layer between the GM and the overlying drainage material has a critical effect on the tensile strains induced in the GM. The number of indentations and maximum strain induced for the different loadings and protection layers examined by Tognon *et al.* (2000) are summarized in Table 5. The best protection for the underlying GM was provided by a sand filled geocushion or a special rubber geomat, which limited strains induced by coarse (40-50 mm) angular gravel to 0.9% at 900 kPa and 1.2% at 600 kPa respectively. Of the protection layers tested, the worst protection was provided by the lowest mass (435 g/m²) nonwoven geotextile which allowed 350 indentations/m² and a maximum strain of 8% at an applied pressure of 250 kPa, and 1200 g/m² of geotextile which allowed about 340 gravel indentations per square metre in the GM and a peak strain (13%) close to the yield strain at 900 kPa. In either case, if only 0.001% of the indentations eventually resulted in a pin hole, this would correspond to over 30 holes/ha.

Table 5 – Summary of number of indentations and peak strains observed in large scale tests using 40-50mm coarse angular leachate collection gravel separated from a 1.5mm geomembrane over compacted clay by various different protection layers (adapted from Tognon *et al.*, 2000).

Protection layer	Mass/area (kg/m ²)	Vertical pressure (kPa)	N. of indentations (#/m ²)	Maximum indentation (mm)	Peak strain (%)
One layer geotextile 1	435	250	350	5.1	8.0
Two layers geotextile 2	1,200	900	338	7.6	13
Sand filled geocushion	2,130	650	69	3.8	0.8
Sand filled geocushion	2,130	900	78	2.9	0.9
Rubber mat	6,000	600	156	3.3	7.5
Rubber mat with polyester scrim	6,000	600	38	1.7	1.2

The two rubber geomats examined were identical except for the presence of a polyester grid reinforcement bonded to the second geomat. The large difference in maximum strains (7.5% and 1.2% respectively at a pressure of 600 kPa) observed for these two geomats suggests that the tensile stiffness provided by the polyester grid played a significant role in reducing lateral deformation of the rubber and hence reducing indentation and strains in the GM. Thus the tensile stiffness of the protection layers may be a critical factor in minimizing strains in GMs.

The tests conducted by Tognon *et al.* (2000) were relatively short-term (200 to 720 min) and at room temperature (24 ± 1 °C). Thus the peak strain may not represent the maximum localized strain that could develop in longer term tests. Additional research is needed to clarify the time dependent effects of strains induced by gravel particles. Nevertheless it is clear that a sand protection layer provides the best potential long-term performance.

7 – WRINKLES IN GEOMEMBRANES

Wrinkles in a GM predominantly arise from thermal expansion when the GM is heated by the sun after placement. Giroud & Morel (1992) performed a theoretical analysis that led to the conclusion that HDPE may be expected to exhibit large wrinkles with heights up to 10 cm and widths up to 30 cm. Rowe *et al.* (2004b) report a case where there were 1200 wrinkles/ha. Some typical wrinkle dimensions observed in the field are summarized in Table 6. Wrinkles are important because of the increased potential for contaminant migration through a hole in the GM at or near the wrinkle. There is also increased potential for development of future holes due to stress cracking at points of high tensile stress in the wrinkle.

Table 6 – Reported HDPE geomembrane wrinkle dimensions.

Wrinkle			Comment	Reference
Width (m)	Height (m)	Spacing (m)		
0.2-0.3	0.05-0.1	4-5	Primary wrinkles parallel to seam between rolls; smaller wrinkles perpendicular to main wrinkles	Pelte <i>et al.</i> (1994)
0.1-0.8	0.05-0.13	0.3-1.6	Wrinkles < 4 m long	Touze-Foltz <i>et al.</i> (2001)
0.3	0.2	-	At the slope to floor transition zone	Davies (pers. comm.)

Chappel *et al.* (2007) have developed a low altitude air photo system that can be used to quantify the geometry of GM wrinkles at a large scale. The system consists of a Digital Single Lens Reflex (DSLR) camera with remote infrared shutter control mounted on a tethered helium blimp (Fig. 6). This system allows the operator to obtain clear, accurate near-vertical air photos (Fig. 7). The wrinkle geometry is analyzed from the low altitude air photos using the digital image processing capabilities and custom functions in Matlab. This allows the user to geometrically correct images; stitch images of parts of a site together into a single image; and select and quantify wrinkle geometry from the image of the site.

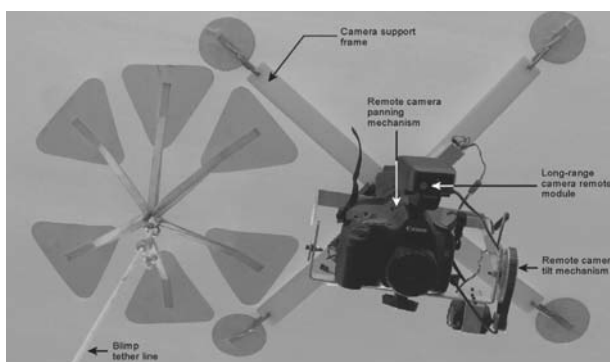


Fig. 6 – Photograph showing digital camera mounted to the underside of the blimp (after Chappel *et al.* 2007).

Inspection of Fig. 7 shows: (A) the seams between GM panels at a spacing of about 6.6 m, (B) wrinkles at a spacing of about 3.4m that run the entire length of the panel along the folds produced during the manufacture of the GM, (C) wrinkles perpendicular to the panel, (D) wrinkles at about

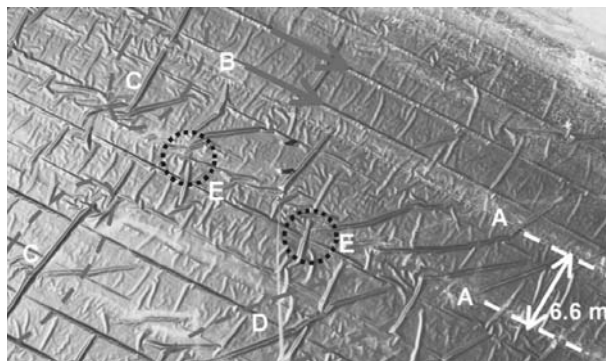


Fig. 7 – Air photo of geomembrane installation. 1.5mm smooth HDPE; Camera elevation 65 m; Latitude 43 °16' N; Air temperature 28 °C; 1:20 pm Aug 18 2006 (modified from Chappel *et al.* 2007).

45 ° to the panel, and (E) the interconnectedness of wrinkles. Since fluid entering a hole in a wrinkle can run along the entire interconnected length, the length of a wrinkle should be regarded as the total linear distance fluid can migrate along a wrinkle and its interconnections. For the site shown, there was about 530 m of wrinkle per hectare and about 420 m of connected wrinkle per hectare. As will be discussed in the section on leakage, the presence of wrinkles can significantly increase the leakage through the composite liner.

7.1 – Behaviour of geomembrane wrinkles under load

The wrinkles formed during placement of the GM do not necessarily disappear when the GM is covered and the waste is placed (Stone, 1984; Soong & Koerner, 1998; Gudina & Brachman, 2006a,b). Compression of these wrinkles due to loading can be expected to induce tensile strains in the GM and these may contribute to the formation of holes due to stress cracking. Gudina & Brachman (2006a,b) examined the interaction between the granular material and the wrinkle using a specially designed apparatus that allows the simulation of the foundation layer, composite liner with a wrinkle in the GM, the protection layer and the granular drainage layer. The system can then be loaded to simulate pressure due to the waste of 1000 kPa (or more). For example, Fig. 8 shows the initial wrinkle shape and the deformed shape of the wrinkle following application of 1000 kPa for a test with sand above and below the GM (SP). Results are also shown for a test with 50 mm gravel above and a GCL beneath the GM

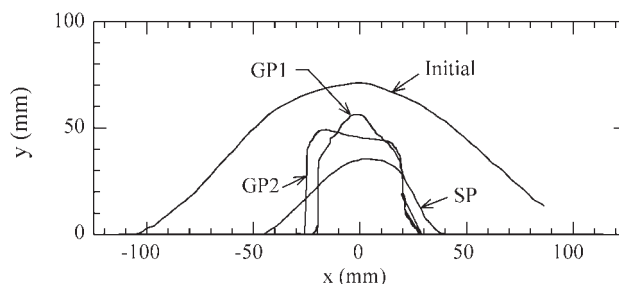


Fig. 8 – Wrinkle geometry in a 1.5 mm HDPE geomembrane before and after application of 1000 kPa vertical pressure for 10 h. Results shown for sand above and below the geomembrane (SP) and 50mm gravel directly above and a GCL beneath the geomembrane at two locations on the wrinkle: GP1 and GP2 (after Rowe *et al.* 2004b).

(GP1 and GP2). The gravel resulted in more severe and nonuniform deformation of the GM than the sand due to the discrete nature of the interactions with the coarse gravel. With gravel there was both pinching (GP1) and flattening at the top (GP2) of the GM which give rise to increased tensions in the GM. This indicates the desirability of having a sand protection layer that is of sufficient thickness to cover the wrinkles between the gravel drainage layer and the underlying GM.

Tests performed by Gudina & Brachman (2006a) found that with a compacted clay subgrade beneath the GM, the gap between an initially 200 mm wide and 60 mm high wrinkle and the CCL could be completely filled with clay if sufficient pressure was applied. The pressures required for this ranged from 100 kPa for a CCL with a water content (16%) at the plastic limit for that clay and 500 kPa for the same clay at a water content (13%) 1% wet of standard Proctor optimum.

The strains induced in the GM with a wrinkle are given in Table 7 for four different protection layers and an applied pressure of 250 kPa. Without protection the strains are very large (42%, which is twice the yield strain) but even with a heavy (1200 g/m²) geotextile protection layer the strains reached 11%. Only the sand protection layer provided low strains (2%) in the GM. Although these tests are for a limited range of conditions, the message that a sand protection layer is far superior to the use of even a thick geotextile protection layer is consistent with other findings described above.

Table 7 – Strains induced in a geomembrane with a wrinkle at an applied pressure of 250 kPa for different protection layers for a configuration comprised of (from top down) nominal 50 mm gravel, protection layer, geomembrane and CCL compacted at the plastic limit (moisture content of 16%). The initial wrinkle was 60 mm high and 240 mm wide (adapted from Gudina & Brachman, 2006b).

Protection layer	Maximum GM strain (%)
None	42
Needle-punched nonwoven GT ($M_A = 390 \text{ g/m}^2$)	15
Needle-punched nonwoven GT ($M_A = 1200 \text{ g/m}^2$)	11
150 mm sand layer	2

GT = geotextile; M_A = mass per unit area.

Gudina & Brachman (2006b) and Dickinson & Brachman (2006) performed tests similar to those discussed above except that instead of a CCL a GCL and sand foundation layer were located below the GM. They found that the GM wrinkle experienced a decrease in height and width when subjected to vertical pressure. However, the gap between the GM and GCL remained for all the tests at applied pressures up to 1000 kPa.

Dickinson & Brachman (2006) focused their attention on the effect of the wrinkle on GCL deformations and the effectiveness of different protection layers to minimize GCL deformations. The thickness of the GCL was found to decrease beside the wrinkle and increase beneath the wrinkle due to lateral extrusion of bentonite into the gap beneath the wrinkle. Without a protection layer the gravel backfill caused bentonite extrusion from beneath gravel contacts to zones in between particles causing large variations in the thickness of the GCL (with a minimum thickness of about 2 mm). More surprising was the finding that the heavy ($M_A = 1200$ and 2000 g/m^2) nonwoven needle-punched geotextile protection layers tested were not effective at reducing the number and magnitude of these indentations. As shown in Figs. 9 and 10, at an applied pressure of 250 kPa, even with a 2000 g/m^2 protection layer there was thinning of the hydrated GCL to as little as 2.2 mm compared to an average initial thickness of 7.8 mm. In contrast, the 150mm thick sand

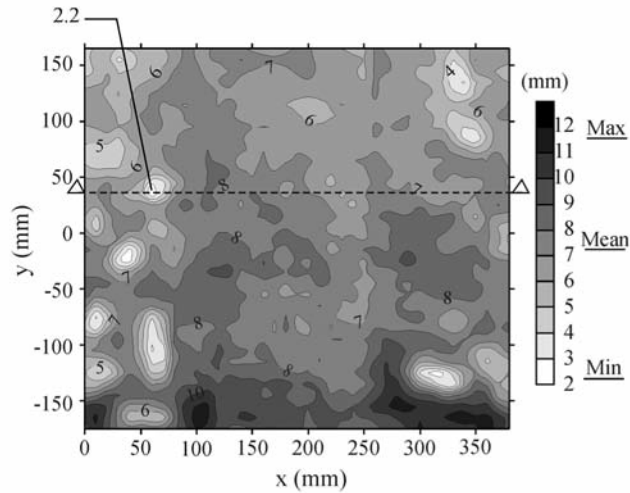


Fig. 9 – Contours of the final thickness of a GCL after application of 250 kPa vertical pressure. Configuration comprised (from top down) nominal 50 mm gravel, for a 2000 g/m² needlepunched nonwoven protection layer, geomembrane and GCL ($w = 115\%$), sand layer (adapted from Dickinson & Brachman, 2006). Marked cross-section shown in Fig. 10.

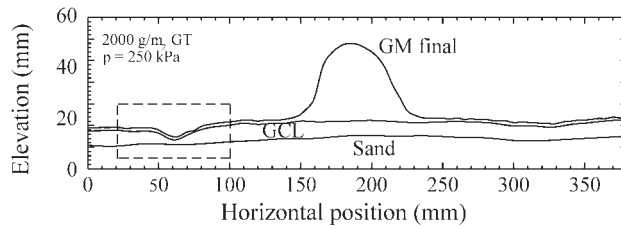


Fig. 10 – Cross-section through Fig. 9 at the location of minimum GCL thickness (adapted from Dickinson & Brachman, 2006).

protection layer reduced both the number and magnitude of local indentations giving a minimum final GCL thickness at 250 kPa of 4.2 mm with the sand layer. The sand protection layer redistributes the gravel contact stresses such that the majority of the GCL deformation was due to consolidation of the bentonite rather than lateral extrusion. As noted by Dickinson & Brachman (2006), this is preferable because a relatively uniform reduction in void ratio from consolidation would be accompanied by a reduction in hydraulic conductivity.

While more research is needed, it appears that in order to provide the best performance of both the GM and GCL used in composite liners, a 150 mm thick sand protection layer is far preferable to even a thick nonwoven needle-punched geotextile (2000 g/m²) on the base of a landfill.

8 – LEAKAGE THROUGH COMPOSITE LINERS

8.1 – Holes in geomembranes

In the absence of holes, a GM is essentially impermeable to water and hence any leakage (advective transport) through GMs must be through holes in the GM. Based on 205 results from

four published leak detection surveys, Rowe *et al.* (2004b) found that: (a) no holes were detected for 30% of the cases; and (b) less than 5 holes/ha were detected for half of the surveys. Nosko & Touze-Foltz (2000) reported 3 holes/ha after installation and 12 holes/ha after placement of drainage layer. Table 8 indicates that 50% of holes in studies reported by Colucci & Lavagnolo (1995) had an area of less than 100 mm² ($r_o < 5.64$ mm). Since the leak detection surveys used to establish the number and size of holes discussed above are conducted shortly after construction of the liner system, it is uncertain how many holes may develop under combined overburden pressures, elevated temperatures and chemical exposure years after construction and placement of the waste. These holes may arise from: (a) indentations at gravel contacts following placement of the waste; (b) stress cracking at points of high tensile strain in wrinkles; and (c) sub-standard seams subjected to tensile stresses.

Table 8 – Reported size of holes in geomembranes
(based on data reported by Colucci & Lavagnolo, 1995).

Leak area (mm ²)	Equivalent radius for circular hole, r_o (mm)	Percentage (%)	Cumulative percentage (%)
0-20	0-2.5	23.2	23.2
20-100	2.5-5.64	26.3	49.5
100-500	5.64-12.6	28.2	77.7
500-1000	12.6-17.8	8.8	86.5
10 ³ -10 ⁴	17.8-56.4	7.8	94.3
10 ⁴ -10 ⁵	56.4-178	4.5	98.2
10 ⁵ -10 ⁶	178-517	1.2	100

8.2 – Calculation of leakage through holes in the geomembrane

Rowe (2005) has provided an extensive discussion of leakage through composite liners based on both theoretical considerations and observed field behaviour and only a brief summary is provided here - the reader is referred to the prior publication for details. At present, the leakage through composite liners is usually calculated using empirical equations (established by curve fitting families of solutions from analytical equations; *e.g.*, Giroud & Bonaparte, 1989; Giroud, 1997; Giroud & Touze-Foltz, 2005; Touze-Foltz & Giroud, 2005). The results obtained from these equations can be compared with the observed leakage through the primary liner at a large number of landfills with double liner systems as reported by Bonaparte *et al.* (2002).

Rowe (2005) made this comparison and concluded that one can not explain the typical observed leakage using the traditional equations and a reasonable number of holes per hectare.

Rowe (1998) presented an analytical solution for the case where a hole coincides with a wrinkle in the GM of length, L , and width, $2b$ (Fig. 11). The transmissivity beneath the wrinkle is much greater than the interface transmissivity, θ , where the GM is in contact with the underlying soil. It is also assumed that $L > b$ such that the effects of leakage at the ends of the wrinkle can be neglected. This solution assumes unobstructed lateral flow along the length, L , and across the width, $2b$, of the wrinkle and then lateral flow between the GM and the soil outside the wrinkle. One dimensional, vertical flow is assumed from the transmissive layer through the underlying soil beneath the wetted

distance from the wrinkle (this is an approximation). Rowe's solution allows consideration of interactions between adjacent similar wrinkles assumed to be spaced at a distance $2x$ apart and the leakage, Q , is given by:

$$Q = \frac{2Lk \left[b + \frac{1 - \exp(-\alpha(x-b))}{\alpha} \right] h_d}{D} \quad (2)$$

where L is the length of the wrinkle; $2b$ is the width of the wrinkle; k is the hydraulic conductivity of the clay liner; θ is the transmissivity of the GM-clay liner interface; $\alpha = [k/(D\theta)]^{0.5}$; h_d is the head loss across the composite liner; and D is the thickness of the clay liner. Assuming no interaction with an adjacent wrinkle, the leakage, Q , is given by:

$$Q = \frac{2L[kb + \sqrt{kD\theta}] h_d}{D} \quad (3)$$

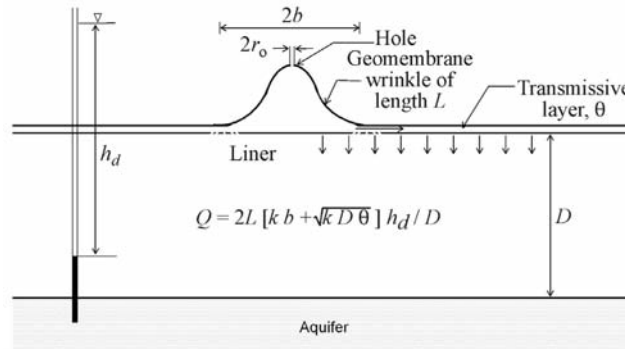


Fig. 11 – Schematic defining leakage through a composite liner with a wrinkle. Assumes lateral migration at interface and vertical flow in clay liner.

The leakage calculated using this wrinkle analytical solution is compared with that from a 2D finite element analysis in Figs. 12 and 13 and again it can be seen that there is excellent agreement between the analytical solution and the 2D numerical analysis with an error of 5% (or less) for both the GM/GCL composite liner (Fig. 12) and GM/CCL composite liner (Fig. 13) for range of cases considered. Figures 12 and 13 also highlight the difference in leakage that would be expected for a hole in direct contact with the clay liner and one in a 15 m long wrinkle.

Table 9 compares the observed and calculated (using Eq. (2) and accounting for interaction assuming equally spacing of the wrinkles) leakage for a GM over a 0.9 m thick CCL. Three different liner conditions were examined: (a) low hydraulic conductivity liner and good interface conditions; (b) typically specified liner and good interface conditions; and (c) typically specified liner and poor interface conditions. The typical range of observed average leakage could be explained by 12 holed (0.2 m wide) wrinkles/ha (3 to 30 m long) with a typical liner and good contact (Case (b)). Similarly Table 10 shows that the observed average leakage of 60-160 lphd could be explained by one holed wrinkle that has a 70-180 m long interconnected length per hectare for Case (b) (based on Eq. (3); *i.e.* assuming the wrinkle is linear).

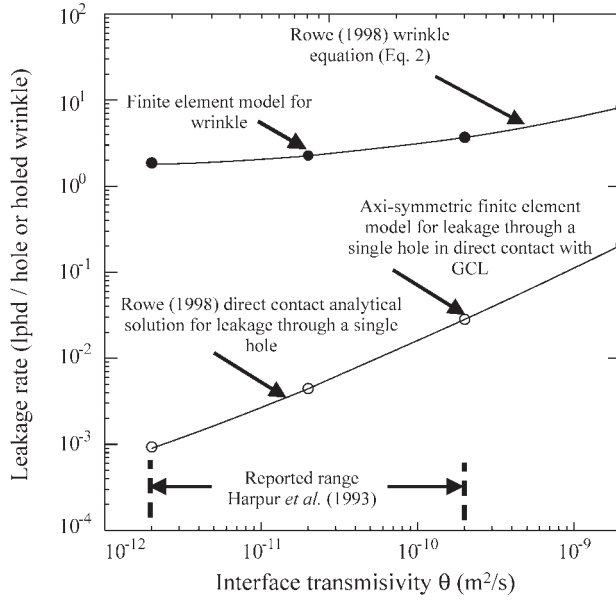


Fig. 12 – Comparison of leakage rates for GM/GCL/attenuation layer composite liner and a range of interface transmissivities as calculated from analytical solutions and FEM analysis for (a) a single hole in direct contact with the GCL and (b) a single 15 m long wrinkle with a hole. $k_L = 5 \times 10^{-11}$ m/s, $H_L = 0.01$ m, $k_f = 1 \times 10^{-6}$ m/s, $H_f = 0.5$ m, $L = 15$ m, $B = 30$ m and $2b = 0.3$ m.

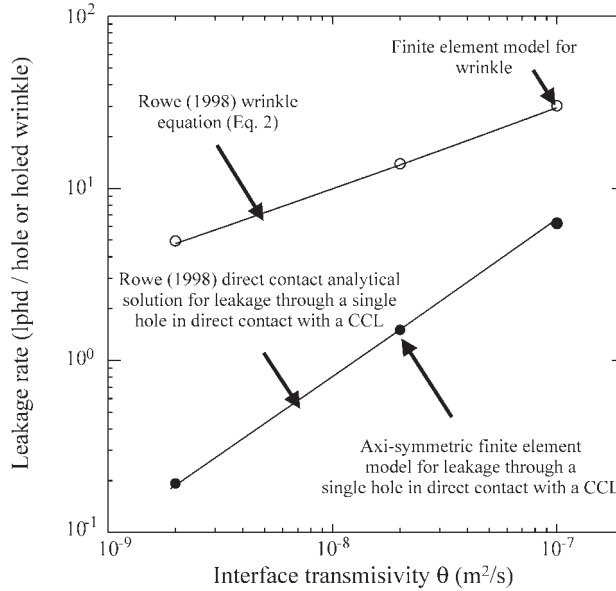


Fig. 13 – Comparison of leakage rates for GM/CCL composite liner and a range of interface transmissivities as calculated from analytical solutions and FEM analysis for (a) a single hole in direct contact with the GCL and (b) a single 15 m long wrinkle with a hole. $k_L = 5 \times 10^{-9}$ m/s, $H_L = 0.51$ m, $L = 15$ m, $B = 30$ m and $2b = 0.3$ m.

Table 9 – Comparison of calculated (with wrinkles) and observed leakage during the active period for 0.9m thick CCL and GCL. k = hydraulic conductivity, θ = interface transmissivity.

Case	Liner	k (m/s)	θ (m ² /s)	Leakage for stated number of holed wrinkles/ha ¹ (lphd)		Observed ² (lphd)	
				2.5	12	Range	Peak ⁴
(a)	0.9 m CCL	1×10^{-10}	1.6×10^{-8}	2-20	10-65	60-160 ³	390 ⁴
(b)	0.9 m CCL	1×10^{-9}	1.6×10^{-8}	7-70	30-310		
(c)	0.9 m CCL	1×10^{-9}	1×10^{-7}	16-160	80-580		
(d)	GCL ⁷	5×10^{-11}	2×10^{-10}	0.6-6	3-30	0.6-1.5 ⁵	54 ⁶
(e)	GCL ⁷	2×10^{-10}	2×10^{-10}	1.6-16	8-75		

Rounded; ¹Range of calculated values corresponds to $L = 3$ and 30 m (accounting for interaction); Hole $r_o = 5.6$ mm; $h_w = 0.3$ m, $h_a = 0$, $2b = 0.2$ m;

²based on data from Bonaparte *et al.* (2002) for systems with a GN LDS;

³Time weighted based on the reported values for different time periods for 4 landfill cells with 900 mm CCL and GN LDS (from Table 4 of Rowe, 2005);

⁴Largest peak value reported for a monitoring period;

⁵Mean of average monthly flows in post-closure and active period;

⁶Largest peak monthly flow reported;

⁷Calculations assume thickness of 0.01 m.

The peak leakage of 390 lphd could be explained by about 1 holed 440 m long interconnected wrinkle/ha and good interface conditions (Table 10). Thus the typical observed leakage for composite liners involving CCLs can be readily explained by holes in wrinkles for a reasonable number of holes/ha.

Table 9 also shows observed leakage and the calculated leakage for two GCL cases: (d) low k GCL (assuming no significant clay-leachate interaction) and (e) high k GCL (assuming significant clay-leachate interaction). Both cases assume the highest interface transmissivity measured by Harpur *et al.* (1993). It can be seen that for the best conditions (Case (d)) about 2.5 holed 3-30 m long wrinkles/ha are needed to explain the typical observed range of 0.6-1.5 lphd. Alternatively this range could be explained by one holed 8-20 m long interconnected wrinkle per hectare (Table 10).

Table 10 – Calculated leakages with one holed wrinkle per hectare for comparison with observed leakages given in Table 9 (after Rowe, 2007).

Case ^{1,2}	Liner	k (m/s)	θ (m ² /s)	Wrinkle length (m)	Leakage (lphd)
(b)	0.9 m CCL	1×10^{-9}	1.6×10^{-8}	70	60
(b)	0.9 m CCL	1×10^{-9}	1.6×10^{-8}	180	160
(b)	0.9 m CCL	1×10^{-9}	1.6×10^{-8}	440	390
(d)	GCL ³	5×10^{-11}	2×10^{-10}	8	0.6
(d)	GCL ³	5×10^{-11}	2×10^{-10}	20	1.5
(d)	GCL ³	5×10^{-11}	2×10^{-10}	670	54
(e)	GCL ³	2×10^{-10}	2×10^{-10}	250	54

¹Corresponds to same cases as examined in Table 9 but only one holed wrinkle and effect of wrinkle length is examined.

² $h_w = 0.3$ m, $h_a = 0$, $2b = 0.2$ m.

³Calculations assume thickness of 0.01 m.

The peak flow of 54 lphd can be explained by good conditions (Case (d)) and one holed 670 m long interconnected wrinkle per hectare or poorer conditions (Case (e)) and one holed 250 m long interconnected wrinkle per hectare (Table 10). Thus the typical observed leakage for composite liners with GCLs also can be readily explained by holes in wrinkles for the typical number of holes/ha and reasonable combinations of other parameters.

The monitoring of flows in the leak detection system can provide insights about when there has been damage to the liner. This may be particularly important when the composite liner is comprised of a GM and GCL. It has been shown that this combination generally gives the less leakage and a GM and CCL. However, unless it is protected by an adequate protection layer or operating procedures, this system is the most prone to damage. Even if a landfill is well constructed, subsequent landfill activity such as moving waste can result in holes through the entire GM/GCL primary liner system. This, in turn, can result in the flow in the leak detection system increasing from the normal values (10 lphd or less) to values several orders of magnitude higher. The advantage of a double lined system is that it allows the detection of these accidents and their repair before too much waste has been placed over the location. With a single lined system it is unlikely that such a breach would be detected until the waste has all been placed and it is no longer practical to repair. This highlights the need to place an adequate protection layer above the composite liner to minimize the risk of such accidental damage. It also highlights the need to closely monitor not only the construction of the liner but also any waste placement or other work that could potentially cause damage to the liner.

There are a number of other factors that can influence the leakage that is observed in the leak detection system of double lined landfills. For example, the interpretation of data for the initial period may be complicated by the contribution of construction water to the measured leakage and interpretation of the data from systems employing CCL layers is complicated by the presence of water that squeezes out of the clay as the load on the clay increases, referred to as consolidation water. However the field cases reported here are all for systems with a geonet leak detection system and there would not be much retained water in these systems. Also Rowe (2005) looked at data for composite liners with CCLs and there was no correlation between leakage and liner thickness as one would expect if consolidation water was representing a significant component of the fluid being collected. Furthermore, the time to for consolidation of typical CCLs is relatively short and the amount of water that would be released more than a few months after loading is quite small and could not explain the leakages reported for CCLs. Thus the most likely explanation for the higher than expected flows based on typical calculations is holes in wrinkles.

Of particular note is the need to design systems involving a geonet leak detection system such that swelling and intrusion (under vertical stress) of any overlying GCL does not compromise the drainage function of the underlying geonet (Shaner & Menoff, 1992; Legge & Davies, 2002).

While the foregoing indicates the necessity of considering holes in wrinkles if one is to reasonably estimate leakage through composite liners (assuming there are wrinkles, as in most cases), it should be emphasized that in the post-closure period the observed leakages (Bonaparte *et al.* 2002) are small. For landfills with composite liners involving a GCL the post closure maximum monthly flow was 10 lphd which corresponds to an advective flux of less than 0.4 mm per year. For landfills with a GM/CCL composite the average peak monthly flow was 60 lphd (*i.e.* an advective flux of about 2mm per year) and in these circumstances contaminant transport is likely to be controlled by diffusion through the liner system for contaminants that can readily diffuse through a GM.

9 – DIFFUSION THROUGH GCL'S AND GEOMEMBRANES

Diffusion is a process wherein contaminants migrate from locations of high concentration (*e.g.* a landfill, lagoon or contaminated groundwater) to a region of lower concentration (*e.g.* clean groundwater). It can occur in air, water, soil or even through solids such as an HDPE GM.

9.1 – Basic concepts associated with diffusion in water and saturated porous media

In its simplest form, molecular diffusion in water is a result of the kinetic activity (random movement) of the atoms (*e.g.* H^+ , Cl^- , Na^+ , Fe^{2+} , Cd^{2+}) or molecules (*e.g.* OH^- , HS^- , HCO_3^- , CH_3COO^- , $Fe(CN)_6^{3-}$, CH_2Cl_2 , C_6H_6 , $C_6H_5C_2H_5$, H_2O , D_2O). The amount of movement is directly proportional to absolute temperature (*i.e.* there is no movement, and hence no diffusion, only at zero degrees Kelvin). At the location where a contaminant enters a body of water there is a high concentration (*i.e.* large number of atoms and/or molecules of the contaminant per unit volume) and thus a high probability that these molecules will collide with other atoms/molecules. As a result of the collision the atoms/molecules are likely to be propelled out of the region of high concentration into a region of lower concentration.

Imagine, as a very crude analogy, the start of a game of billiards where there is an initial collection of balls at one location on a billiard table. As the cue ball is driven into the collection of balls, the energy imparted by the collision causes the balls to spread out around the table reducing the concentration around the initial location of the clustering of balls. Assuming no balls fall into the pockets in the table, further play is likely to cause further spreading of the balls.

The diffusion coefficient of a given contaminant in water is a complex function of the mass, radius, valence, and concentration/dissociation state of the contaminant, and the viscosity, dielectric constant and temperature of the diffusing medium (water in this case). The presence of soil particles, particularly clay minerals and organic matter, complicates the diffusion process. Diffusion through a network of clay particles (or fibres in a geotextile for the geotextile component of a GCL) involves the diffusive movement of the species of interest in the pore water between the clay particles (or geotextile fibres). There are many complicating factors that affect the diffusion of contaminants through water in the pores of a saturated porous medium (see Chapter 6 of Rowe *et al.* 2004b for a detailed discussion). However for most practical purposes these can be represented in terms of the effective porosity, n , of the medium and an effective diffusion coefficient, D_e . The greater the porosity, the more the pore water (per unit volume) available for diffusion to occur and, hence, the greater the diffusive flux of contaminant (other things being equal). Techniques for establishing the effective diffusion coefficient and their limitations are described by Rowe *et al.* (2004b).

The migration of certain organic contaminants can be retarded by adsorption and/or absorption onto organic matter in the soil or polymer fibres for a needle punched GCL. Another completely different mechanism involves cation exchange between certain ionic contaminants (*e.g.* NH_4^+ , K^+ , Mg^{2+} , Fe^{2+} etc) and clay soils (*e.g.* bentonite in a GCL) and this results in a similar reduction in concentration. Since the precise details of the mechanism are not important for most practical purposes, adsorption, absorption and cation exchange are often lumped together and referred to as “sorption”. Historically, sorption parameters are obtained from batch tests where a given mass of soil is added to a solution with a known initial concentration of the contaminant of interest. There is then a partitioning of the contaminant between the dissolved phase (*i.e.* in the solution) and the soil. At the point of chemical equilibrium, a partitioning coefficient, K_d , can be deduced. Assuming low concentrations of contaminant, the partitioning coefficient will be a constant for a given contaminant

and soil and, as a consequence, the mass of contaminant sorbed onto the soil per unit mass of the soil, C [-], will be a linear function of the concentration, c [ML⁻³], in the pore fluid:

$$C = K_d c \quad (4)$$

where K_d is called the partitioning or distribution coefficient [M⁻¹L³]. More complicated cases (*e.g.* non-linear sorption) are described by Rowe *et al.* (2004b). It should be noted that for organic contaminants the actual mechanism associated with sorption onto organic matter in soil or the geotextile fibres in a GCL involves (a) partitioning of contaminant between the pore fluid and the surface of the solid, and (b) diffusion into the solid organic matter or geotextile fibre. Thus, while it takes some time to reach equilibrium, the time scale is generally short relative to the time scale of the diffusion through the porous medium because the particles are very small (thin, in the case of geotextile fibres) and thus is modelled as instantaneous. The processes involved in sorption of organic contaminants here are similar to those described below for diffusion through GMs. The difference is that in the case of diffusion into organic matter or geotextile fibres in the soil, the contaminant is being removed from solution in a situation where the primary path for diffusion is in the pore fluid and thus it ceases to participate in diffusion from source to receptor (unless the concentration in the pore fluid drops, in which case it can be slowly released back into solution for reversible sorption). In the case of an intact GM discussed below, the only way for the contaminant to diffuse from pore fluid on one side of the GM (*e.g.* source) to that on the other side (*e.g.* receptor) is for the contaminant to diffuse through the GM.

Radioactive contaminants and some organic contaminants will also experience a decrease in concentration due to radioactive decay or biodegradation. This can often be represented in terms of first order decay where the rate of reduction of concentration, dc/dt , is proportional to the current concentration, c , so that:

$$\frac{dc}{dt} = -\lambda c \quad (5)$$

where λ is the first order decay constant [T⁻¹].

The factors discussed above can be combined and the contaminant transport through the soil component of barrier systems can be modelled by solving the equation for one-dimensional contaminant transport of a single reactive solute through a porous medium (Rowe *et al.*, 2004b):

$$n \frac{\partial c}{\partial t} = n D_e \frac{\partial^2 c}{\partial z^2} - \rho_d K_d \frac{\partial c}{\partial t} - \lambda c \quad (6)$$

subject to appropriate boundary and initial conditions, where c is the concentration at depth z and time t ; n is the effective porosity; D_e is the effective diffusion coefficient; ρ_d is the dry density of the medium through which diffusion takes place; K_d is the partitioning coefficient; and λ is the first order decay constant. Typically, diffusion parameters are inferred from laboratory tests conducted using the soil of interest and a leachate similar to that anticipated in the field application. While the diffusion coefficient may vary from soil to soil and case to case, it usually falls within a much narrower range than hydraulic conductivity.

9.2 – Diffusion through unsaturated soils

For non-volatile contaminants which will readily diffuse through water but not air, unsaturated soil provides a better diffusion barrier than a saturated soil since they can only diffuse through the

water phase. Equations for estimating the diffusion coefficient for unsaturated soils are given by Rowe *et al.* (2004b). For volatile contaminants the opposite is true. Volatile organic contaminants (VOCs) such as dichloromethane (DCM), 1,2 dichloroethane (DCA), trichloroethene (trichloroethylene, TCE), benzene, toluene, ethylbenzene, m&p-xylene and o-xylene will diffuse orders of magnitude faster in a dry soil than they will through a saturated soil. In an unsaturated soil, they will diffuse in both the gaseous and dissolved phases, but diffusion will be predominantly through the gas filled pores if the water content is low enough to have a significant number of continuous gas filled pores. This issue is addressed in more detail by Rowe *et al.* (2004b), however it is worth noting here that for double liner systems, even if there is no leachate in contact with a primary or secondary GM liner, VOCs in the gaseous phase in the leachate collection system will readily diffuse through typical primary composite liners, an unsaturated leak detection system, and the secondary GM with the secondary liner and attenuation layer providing the most significant resistance to their migration.

9.3 – Diffusion through hydrated GCLs

There is a direct correlation between the diffusion coefficient and the bulk void ratio of the GCL and Lake & Rowe (2000) showed that the chloride diffusion coefficient ranged between $1 \times 10^{-10} \text{ m}^2/\text{s}$ ($0.003 \text{ m}^2/\text{a}$) and $4 \times 10^{-10} \text{ m}^2/\text{s}$ ($0.013 \text{ m}^2/\text{a}$) for the range of conditions they examined. This may be compared with a typical diffusion coefficient of about $6 \times 10^{-10} \text{ m}^2/\text{s}$ ($0.02 \text{ m}^2/\text{a}$) through a CCL. Lake & Rowe (2004) reported diffusion coefficients of between about $2 \times 10^{-10} \text{ m}^2/\text{s}$ ($0.006 \text{ m}^2/\text{a}$) to $3 \times 10^{-10} \text{ m}^2/\text{s}$ ($0.009 \text{ m}^2/\text{a}$) for several VOCs (DCM, DCA, TCE, benzene and toluene) through a GCL at room temperature and a confining pressure less than 10 kPa. Rowe *et al.* (2005b) extended this work by examining the effect of temperature on the diffusion of benzene, toluene, ethylbenzene, m&p-xylene and o-xylene (BTEX). They showed that the geotextile component of a GCL was the primary contributor to sorption of hydrocarbons by the GCL, and partitioning coefficients (K_d at 22 °C and 7 °C in mL/g) for the entire GCL were: m&p-xylene (42, 25) > ethylbenzene (36, 22) > o-xylene (27, 14) > toluene (15, 8.7) > benzene (4.4, 2.6). The diffusion coefficients (at 22 °C and 7 °C in m^2/s) followed the order benzene (3.7×10^{-10} , 2.2×10^{-10}) > toluene (3.1×10^{-10} , 1.8×10^{-10}) > ethylbenzene (2.9×10^{-10} , 1.7×10^{-10}) > m&p-xylene (2.5×10^{-10} , 1.5×10^{-10}) \approx o-xylene (2.6×10^{-10} , 1.5×10^{-10}). While the change in temperature from 22 °C to 7 °C reduced both the diffusion and sorption coefficients, these reductions had opposite effects on mass transport through the GCL with the decrease in mass transport due to a reduced diffusion coefficient dominating over the increase due to smaller sorption. Thus the net effect was less mass transport at lower temperature.

9.4 – Diffusion through geomembranes and composite liners

Although the basic mechanism causing molecular diffusion is the same as for a porous medium (*e.g.* GCL, CCL or underlying subsoil), the details of how diffusion occurs through a “solid” GM are somewhat different. In the case of the saturated porous medium the diffusion occurs in the pore water between the solids (be they soil particles or geotextile fibres) and sorption onto the soil particles or geotextile fibres serves to remove contaminant from the pores and hence from impact on an underlying receptor. In the case of a solid GM, sorption (partitioning) onto the polymer is an essential first step that attaches the contaminant to the plastic and provides an initial concentration for diffusion through the GM (Fig. 14). It needs to be remembered that while a GM is a solid, at the molecular level it is made up of chains of polymers that are vibrating (with the amount of vibration being a function of temperature) and there is space between these polymer

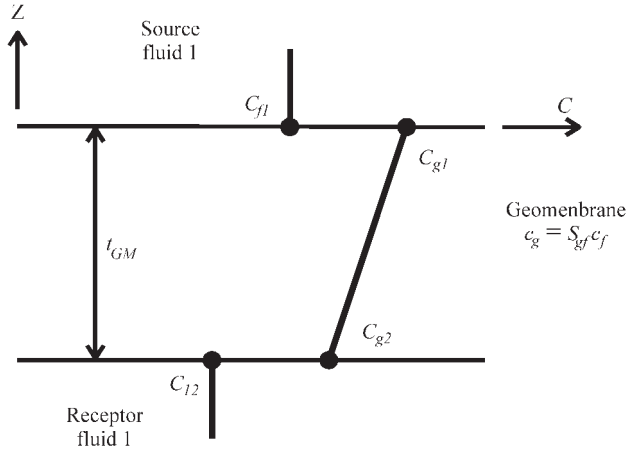


Fig. 14 – Concentration profile for diffusion across a geomembrane showing (a) partitioning between the concentration in the source solution, c_{f1} , and the concentration in the adjacent geomembrane, c_{g1} ; (b) diffusion profile from the top to bottom of the geomembrane; (c) partitioning between the concentration at the bottom of the geomembrane, c_{g2} and the concentration in the receptor solution, c_{r2} . Note that $c_{g1}/c_{f1} = c_{g2}/c_{r2} = S_{gf}$.

chains which, although not visible to us, may be significant with respect to the size of contaminant atoms or molecules. Thus the diffusion of contaminants through an intact GM is a molecule activated process that can be envisioned to occur by steps or jumps over a series of potential barriers, following the path of least resistance. For dilute aqueous solutions, the process involves three key steps (Haxo & Lahey, 1988) as illustrated in Fig. 14: (i) partition of the contaminant between the medium containing the contaminant and the inner (*i.e.* contacting) surface of the GM (sorption); (ii) diffusion of the permeant through the GM; and (iii) partition between the outer surface of the GM and the outer medium (desorption). The diffusive motion depends on the energy availability and the relative mobilities of the penetrant molecules and polymer chains. This will depend on temperature, the size and shape of the penetrant, the nature of the polymer and, potentially, concentration.

The extent to which permeant molecules are sorbed in a polymer depends upon the activity of the permeant within the polymer at equilibrium (Müller *et al.*, 1998). When a GM is in contact with a fluid, there will be a relationship between the final equilibrium concentration in the GM, c_g , and the equilibrium concentration in the fluid, c_f where the concentrations c_f and c_g represent the amount of the substance of interest (contaminant) dissolved per unit volume of the water or GM respectively. The concentration is typically represented in terms of mol per litre (mol L^{-1}) or as a mass concentration in mg/L or $\mu\text{g/L}$. For the simplest case where the permeant does not chemically interact with the polymer (*e.g.*, as is the case for dilute solutions such as typical landfill leachates and HDPE), the relationship between the concentration in the fluid and the GM is given by (Henry's law):

$$c_g = S_{gf} c_f \quad (7)$$

where S_{gf} is called a partitioning coefficient and in principle is a constant for the given molecule, fluid, GM, and temperature of interest. Note that S_{gf} greater than 1 implies a preference for the GM (*i.e.* the amount of substance per unit volume of the GM is greater than that per unit volume of the fluid). This is typically the case for hydrophobic organic contaminants (*i.e.* those with low

solubility in water) which can readily dissolve in HDPE, with the value of S_{gf} being greater the more hydrophobic the contaminant. Thus S_{gf} for ethylbenzene is greater than for benzene which is greater than for dichloromethane (Table 11). Conversely hydrophilic contaminants (*i.e.* those highly soluble in water, like salts such as NaCl) do not readily dissolve in HDPE and have a value of S_{gf} which is less than unity (see chloride in Table 11) since, at equilibrium, most of the substance will be dissolved in the water rather than the GM.

Table 11 – Time to establish steady state diffusion through HDPE geomembrane for three volatile organic compounds.

Contaminant	Diffusion parameters		Time to reach steady state (years)	
	D_g (m ² /a)	S_{gf} (-)	1.5 mm GM	2.5 mm GM
Dichloromethane, CH ₂ Cl ₂	2 x 10 ⁻⁵	6	0.11	0.3
Benzene, C ₆ H ₆	1.3 x 10 ⁻⁵	30	0.16	0.4
Ethylbenzene, C ₆ H ₅ C ₂ H ₅	5.7 x 10 ⁻⁶	285	0.36	1
Chloride, Cl ⁻	1.3 x 10 ⁻⁶	0.0008	1.6	4.4

All numbers have been rounded. Note parameters for chloride represent an upper bound and hence the times shown here are lower bounds (actual time is expected to be longer than shown).

In the second stage of the migration, diffusion of the sorbed penetrant within the GM can be described by Fick's first law:

$$f = -D_g \frac{dc_g}{dz} \quad (8)$$

where, f is the mass flux, D_g is the diffusion coefficient of the considered contaminant in the GM, c_g is the concentration of diffusing substance in the GM, and z is the direction parallel to the direction of diffusion. In transient state, the governing differential equation is (Fick's second law):

$$\frac{\partial c_g}{\partial t} = D_g \frac{\partial^2 c_g}{\partial z^2} \quad (9)$$

which must be solved for the appropriate boundary and initial conditions.

The last stage in the migration process is permeant desorption from the GM to the outer solution. This stage is similar to the first except that here contaminants will diffuse from the GM into the adjacent fluid so that at equilibrium the contaminant concentration in the adjacent fluid is related to that in the GM by the relationship:

$$c'_g = S'_{gf} c'_f \quad (10)$$

where S'_{gf} is the contaminant partitioning coefficient between the outside fluid and the GM. In the simplest case where the solutions on either side of the GM are aqueous, these two partitioning coefficients may be assumed to be the same ($S_{gf} = S'_{gf}$). The two partitioning coefficients described by Eqs. (7) and (10) are conceptually similar to that described for a porous medium by Eq. (4) and can also be obtained in a similar way from batch tests. The parameter differs in detail because of the difference between a porous media and a solid GM and the fact that in the soil, partitioning and the related sorption removes contaminant from the diffusion process through the porous medium while for a solid GM partitioning is associated with the contaminant entering and exiting the GM, with it diffusing through the GM.

Since the primary interest is in the concentrations of contaminant in water (not the GM) it is convenient to express the diffusion equations in terms of the concentration in adjacent solutions cf. Substituting Eq. (7) into Eq. (8), the flux from an aqueous solution on one side of the GM to an aqueous solution on the other side is given by:

$$f = -D_g \frac{dc_g}{dz} = -S_{gf} D_g \frac{dc_f}{dz} - P_g \frac{dc_f}{dz} \quad (11)$$

where the permeation coefficient (called the permeability in the polymer literature), P_g , is given by:

$$P_g = S_{gf} D_g \quad (12)$$

and where P_g is a mass transfer coefficient that takes into account the partitioning and diffusion processes. There are various methodologies that can be used (Rowe, 1998) to deduce the partitioning, diffusion and permeation coefficients.

The permeation coefficient, P_g , is highly dependent on the similarity of the penetrant and polymer. For example, Eloy-Giorni *et al.* (1996) indicated values of $S_{gf} = 8 \times 10^{-4}$ and $D_g = 2.9 \times 10^{-13} \text{ m}^2/\text{s}$ giving a very low value of $P_g = 2.3 \times 10^{-16} \text{ m}^2/\text{s}$ for water and HDPE. Similarly, August & Tatzky (1984) found that strongly polar penetrant molecules have very low permeation coefficients through polyethylene (with the permeation coefficients being in the following order: alcohols < acids < nitroderivatives < aldehydes < ketones < esters < ethers < hydrocarbons). August *et al.* (1992) found that there was negligible diffusion of heavy metal salts (Zn^{2+} , Ni^{2+} , Mn^{2+} , Cu^{2+} , Cd^{2+} , Pb^{2+}) from a concentrated (0.5 M) acid solution (pH = 1-2) through HDPE over a 4 year test period.

Hydrocarbons can readily diffuse through HDPE GMs, although the permeation coefficient will vary depending on factors such as the crystallinity of the GM, temperature and in some cases, the chemical composition and concentrations in the contaminant source (Sangam & Rowe, 2001). The diffusion of hydrocarbons such as benzene, ethylbenzene, toluene and xylenes can also be reduced by a factor of between about 2 and 5 by using a fluorinated HDPE as an alternative to a conventional GM (Sangam & Rowe, 2005).

Rowe (2005) reported on chloride diffusion tests where a source and receptor are separated by a 2 mm thick HDPE GM. After about 12 years, the receptor concentration remained below about 0.02% of the source concentration and lies within the range of analytical uncertainty for the chemical analysis. This data provides an upper bound of $3 \times 10^{-17} \text{ m}^2/\text{s}$ on the permeation coefficient of chloride through an HDPE GM ($D_g = 4 \times 10^{-14} \text{ m}^2/\text{s}$ or $1.3 \times 10^{-6} \text{ m}^2/\text{a}$, $S_{gf} = 0.0008$).

The time it takes to establish steady stage diffusion through an HDPE GM from a constant source to zero concentration receptor can be obtained by solving Eq. (9) subject to these boundary conditions and only depends on the diffusion coefficient D_g (i.e. it does not depend on the partitioning coefficient S_{gf}). The time it takes to reach steady state is given in Table 11 for a number of contaminants and 1.5 and 2.5 mm thick GMs. It can be seen that increasing the thickness of the GM increases the time to reach steady state by about a factor of 2.8 (i.e. by the ratio of the square of the thicknesses = $2.5^2/1.5^2$) but even so, for the three hydrocarbons considered, the time is a year or less. Even for chloride it is less than 5 years. However this highlights the fact that the time to reach steady state diffusion only tells a small part of the story since it only depends on D_g and says nothing about the mass flux that is transported from the contaminant source across the GM which also depends on S_{gf} (see Eq. (11)). The impact that this has is illustrated below.

Table 12 summarizes the calculated time required for contaminant to diffuse through an HDPE GM and increase the concentration, c , in a 1 cm thick receptor to the specified levels relative to the constant source concentration c_o for two GM thicknesses and three hydrocarbons (using the diffusion parameters given in Table 11). It can be seen that it takes 3 to 17 days for the concentration in the receptor to reach 0.1% of the source and only 12 to 55 days to reach 10%. In contrast, Table 13 shows that it would take at least 15 years for chloride to reach 0.1% for a 1.5 mm HDPEGM and at least 1500 years to reach 10% of the source concentration. This highlights how effective the GM is as a diffusion barrier to ions like chloride.

Table 12 – Time required for contaminant to diffuse through HDPE geomembrane and increase the concentration, c , in a 1 cm thick receptor to the specified level relative to the constant source concentration c_o (in percent) for two geomembrane thicknesses.

c/c_o (%)	Time to reach c/c_o in receptor (days)					
	DCM		Benzene		Ethylbenzene	
	1.5 mm	2.5 mm	1.5 mm	2.5 mm	1.5 mm	2.5 mm
0.01	2	5	2	6	5	13
0.1	3	7	3	9	6	17
1	5	12	5	14	10	27
10	12	28	12	30	20	55

All numbers have been rounded.

Table 13 – Time required for chloride to diffuse through HDPE geomembrane and increase the concentration, c , in a 1 cm thick receptor to the specified level relative to the constant source concentration c_o (in percent) for 1.5 mm HDPE GM ($D_s = 1.3 \times 10^{-6} \text{ m}^2/\text{a}$; $S_{gr} = 0.0008$).

c/c_o (%)	Time to reach c/c_o in receptor (days)
0.1	15
1	150
10	1500

All numbers have been rounded; Note parameters for chloride represent an upper bound and hence the times shown here are lower bounds (actual time is expected to be longer than shown).

To give a sense of the rate of diffusive migration, Table 14 summarizes the calculated distance dichloromethane would diffuse in given time periods. This case considers diffusion from a constant source (c_o) through a 1.5 mm HDPE GM, 8.5 mm thick GCL and underlying subgrade. It assumes no sorption in the GCL or soil and thus represents an upper limit to the extent of migration likely to be observed. The distance at which the concentration reaches a given concentration level ($c/c_o = 0.01, 0.1$ and 0.5) is shown together with an apparent “velocity” of diffusion (the distance divided by the time). It can be seen that within a year DCM could diffuse to the 1% level ($c/c_o = 0.01$) to a depth of up to 0.44 m and in 10 years it would migrate more than 1.5 m. The “velocity” of migration is fastest at low times when the concentration gradient is greatest and decreases with subsequent time. It was found that DCM diffusion was not significantly slower when there was no GM. For example in 1, 2 and 4 years, DCM migrated at the $c/c_o = 0.01$ level to depths of 0.5 m, 0.72 m and 1.03 m with no GM as compared with 0.44 m, 0.66 m and 0.96 m with a GM. The reduction in the distance is a little more significant for contaminants for which S_{gr} is higher.

Table 14 – Diffusive migration of dichloromethane through composite GM/GCL liner and underlying subgrade. Depth to location where $c/c_o = 0.01, 0.1$ and 0.5 and corresponding apparent “velocity” of the diffusion front.

Time (years)	$c/c_o = 0.01$		$c/c_o = 0.1$		$c/c_o = 0.5$	
	Depth (m)	“Velocity” (m/a)	Depth (m)	“Velocity” (m/a)	Depth (m)	“Velocity” (m/a)
1	0.44	0.44	0.26	0.26	0.06	0.06
2	0.66	0.33	0.39	0.20	0.12	0.06
4	0.96	0.24	0.59	0.15	0.2	0.05
6	1.19	0.20	0.74	0.12	0.26	0.043
8	1.4	0.18	0.84	0.11	0.31	0.039
10	1.55	0.16	0.96	0.096	0.36	0.036
15	1.92	0.13	1.2	0.08	0.45	0.03
20	2.22	0.11	1.4	0.07	0.53	0.027
25	2.5	0.1	1.56	0.062	0.6	0.024
30	2.74	0.091	1.72	0.057	0.66	0.022
40	3.19	0.080	2	0.05	0.78	0.020
50	3.57	0.071	2.25	0.045	0.87	0.017

GM: 1.5mm $D_g = 1.3 \times 10^{-6} \text{m}^2/\text{a}$; $S_{gf} = 6$; GCL: 8.5mm $D = 0.009 \text{m}^2/\text{a}$, $n = 0.7$; Attenuation Layer 4m, $D = 0.02 \text{m}^2/\text{a}$, $n = 0.3$ no sorption or decay; constant source.

Similar calculations for chloride show no migration below the GM at the 0.01 level for thousands of years. This is because what does diffuse through the GM diffuses away in the underlying soil because of the very low flux through the GM and the much higher diffusion coefficient in the underlying soil. This again highlights the effectiveness of a GM as a diffusion barrier.

For landfill with double liner systems, the leakage through the primary liner will be mostly collected by the leak detection system. This will minimize the potential for advective movement through the secondary liner. However volatile organic compounds (VOCs) will volatilize in the LDS and can then diffuse through the underlying secondary composite liner, and hence diffusion still needs to be considered for these cases. The time for VOCs to migrate through the primary liner at detectable levels will depend on the thickness of the primary liner (*e.g.* see Table 14). Evidence suggesting the likely diffusion of VOCs through geosynthetic liners arises from field observations reported by Workman (1993), Othman *et al.* (1996), and Shackleford (2005). There are other, as yet unpublished, examples of migration through CCLs.

In summary, HDPE GMs are an excellent diffusion barrier to water and water soluble contaminants such as metal salts. However, they will allow diffusion of VOCs. Control of the migration of these compounds will depend on the clay liner and any attenuation layer between the GM and any receptor aquifer. Additional control can be provided by using a fluorinated HDPE GM.

10 – SERVICE LIFE OF GEOMEMBRANES

10.1 – Geomembranes for MSW landfills

The foregoing sections have demonstrated that even with typical wrinkles and holes in wrinkles, provided there is appropriate construction quality control and construction quality

assurance (CQC/CQA), the leakage through composite liners can be controlled to such low values that diffusion becomes the controlling transport mechanism. Geomembranes are also excellent diffusion barriers to ions (like chloride and heavy metals) and the while volatile organic compounds can readily diffuse through the GM they can be controlled by design of the barrier system with an adequate attenuation layer (Rowe *et al.*, 2004b; Rowe, 2005). This all assumes that the GM is performing as designed. However GMs will have a finite service life and their long-term performance will depend on their properties (*e.g.* stress crack resistance, crystallinity, and oxidative induction time), the tensile strains induced by the overlying drainage material and wrinkles (as discussed earlier), the exposure to chemicals in the leachate and temperature. This has been discussed in some detail by Rowe (2005).

It is generally recognized that the chemical ageing of an HDPEGM has three distinct stages (Viebke *et al.*, 1994; Hsuan & Koerner, 1998): (a) depletion time of antioxidants; (b) induction time to the onset of polymer degradation; and (c) degradation of the polymer to decrease some property (or properties) to an arbitrary level (*e.g.* to 50% of the original value). It has been reported that the consumption of antioxidants and subsequent oxidation reaction in polyethylene can be increased in the presence of transition metals (*e.g.* Co, Mn, Cu, Pd and Fe) present in leachate (Osawa & Saito, 1978; Wisse *et al.*, 1990; Hsuan & Koerner, 1998). Since it is not practical to establish the service life under actual field conditions, accelerated ageing tests are conducted at elevated temperatures and the results are then used to calculate the expected service life at the temperatures expected at the base of a landfill (*e.g.* Hsuan & Koerner, 1998; Sangam & Rowe, 2002; Mueller & Jacob, 2003; Rowe, 2005).

In most cases this testing to assess ageing of GMs has involved immersing samples in a fluid of interest and then, after different periods of immersion, samples are removed and tested to obtain the oxidative induction time (OIT). The $\ln(OIT)$ is then plotted versus the period of incubation (Fig. 15). The linear plot implies a first order relationship between OIT and time and hence the OIT (an indicator of the total amount of antioxidants) remaining at time t can be given by:

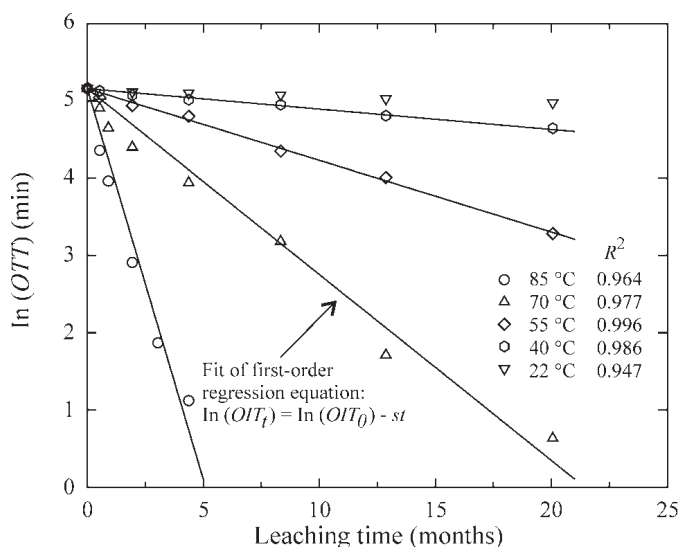


Fig. 15 – Variation in $\ln(OIT)$ with time at different temperatures in leachate. OIT_0 is the initial OIT and OIT_t is the OIT at time t (month), s is the antioxidant depletion rate (month^{-1}) (after Islam & Rowe, 2007).

$$OIT(t) = OIT_o e^{-st} \quad (11)$$

where OIT_o is the initial OIT value (typically in minutes) and s the rate of antioxidants depletion (typically in month⁻¹).

Sangam & Rowe (2002) examined the depletion of antioxidants in air, water and simulated MSW leachate while Rowe (2005) and Rowe & Rimal (2007) reported results for simulated liner systems with a collection layer over the geotextile protection layer, the GM and a GCL on a sand subgrade. Based on the laboratory data and Arrhenius modelling, the time required for antioxidant depletion was deduced and is given in Table 15 for the GMs tested. It can be seen that the exposure conditions and temperature have a profound effect on the time to antioxidant depletion. In particular it is noted that there is a significant difference between immersion in water and leachate. Islam & Rowe (2007) have demonstrated that the primary factor affecting this difference is the presence of surfactant in the leachate. Volatile fatty acids and ions typically found in leachate (e.g. Na, Cl etc) had no significant effect on the time to antioxidant depletion.

Table 15 – Estimated antioxidant depletion time for an HDPE geomembrane (modified from Rowe 2005).

Temperature (°C)	Air ¹ t_{air} (years)	Water ¹ t_{water} (years)	Leachate ¹ $t_{leachate}$ (years)	Simulated liner ² t_d (years)
10	510	235	50	280
20	235	110	25	115
30	110	55	15	50
35	80	40	10	35
40	55	30	8	25
50	30	15	5	10
60	15	8	3	6

All times greater than 10 have been rounded to nearest 5 years. ¹2 mm HDPE, $OIT_o = 133$ min (ASTM D3895), crystallinity = 44%; based on data from Sangam & Rowe (2002). ²1.5 mm HDPE, $OIT_o = 135$ min (ASTM D3895), crystallinity = 49%.

The simulated liner results presented in Table 15 represent only the first stage of the service life. To obtain estimates for Stages 2 and 3, Rowe (2005) used data obtained by Viebke *et al.* (1994) for polyethylene gas pipe with minimal antioxidant and a wall thickness comparable to a GM thickness (2.1 mm). The antioxidant depletion times (Stage 1) for the simulated liner (Table 15) were combined with the service life projections for Stages 2 and 3 based on the activation energies given by Viebke *et al.* (1994) to obtain the “unadjusted” estimates of GM service life given in Table 16. Since Viebke *et al.* (1994) tests were with water on the inside and air on the outside of the pipe wall, the unadjusted values may be expected to overestimate the service life of a GM in a landfill. Thus these values were adjusted to reflect the observed difference between exposure to air, water and a simulated liner exposed to leachate on one side as described by Rowe (2005) to obtain the “adjusted” estimates given in Table 16. It can be seen that for temperatures around 20 °C, service lives are projected to be of the order of 565 to 900 years and hence a service life of 600 years (or more) could be anticipated at a temperature of 20 °C (or less). For liners at a temperature of 35 °C, the service life is of the order of 130-190 years. Finally at temperatures of 50-60 °C, the service lives are very short (15-50 years).

In the context of the earlier discussion of the effect of temperature on primary and secondary liners, it should be noted that for an area where the background temperature is 15 °C and assuming the primary GM temperature increases to 35 °C (*i.e.* by 20 °C), the secondary GM might be expected to be at about 30 °C (assuming a primary composite liner with a GM, 0.75 m compacted

Table 16 – Estimated service lives for an HDPE geomembrane for a MSW landfill
(modified from Rowe 2005).

Temp (°C)	Service life (years) Unadjusted t_{SL}	Service life (years) Adjusted t_{SLa}
20	900	565
30	315	205
35	190	130
40	120	80
50	50	35
60	20	15

All times have been rounded to nearest 5 years.

clay and an 0.3 m thick gravel leak detection system). Under these circumstances Table 16 suggests that the service life of the primary and secondary GMs would be of the order of 130-190 years and 205-315 years respectively.

The service lives presented in Table 16 provide a general idea of the order of magnitude of the GM service-life and highlight the importance of liner temperature. While these numbers represent the best currently available information they should be used with caution since only the results for Stage 1 are based on actual tests on GMs typically used in landfill applications in a simulated liner configuration.

The calculated antioxidant depletion times (Table 15) and service lives (Table 16) are based on a constant temperature. Rowe (2005) examined the effect of the liner temperature varying with time. This showed that while operational features such as operating a landfill as a bioreactor may shorten the period of high temperatures on the liner, the increase in temperature associated with this mode of operation can actually decrease the overall service life. This highlights the importance of considering the mode of landfill operation when developing a liner design.

10.2 – Geomembranes in contact with neat hydrocarbons

As indicated in the previous section, the fluid in contact with the GM can have a profound impact on the depletion of antioxidants and hence the service life of a GM. Since GMs may be used to retain neat hydrocarbons, as discussed earlier, Rowe *et al.* (2007b) immersed both conventional HDPE and fluorinated HDPE (f-HDPE) GM specimens in Jet A-1 and then examined the change in oxidative induction time with the period of immersion. They reported that immersion in Jet A-1 accelerated antioxidant depletion relative to that observed in water or MSW leachate by Sangam & Rowe (2002). Fluorination of the HDPE GM significantly (by a factor of 2.7) reduced antioxidants depletion relative to conventional HDPE. At 23 °C, the total antioxidant depletion time was estimated to be about 2 and 6 years for untreated and fluorinated GMs respectively. This can be compared with projected depletion times of between 20 years and 90 years (at 23 °C) based on Sangam & Rowe's (2002) tests for GM immersed in MSW leachate and water respectively.

11 – CONCLUSIONS

Over the last decade there have been significant advances in knowledge concerning the factors potentially affecting the performance of GCLs and GMs in a wide range of geoenvironmental

applications. This paper has examined nine of these issues and it can be concluded that for the specific materials and conditions discussed:

- GCLs may interact with municipal solid waste (MSW) leachate. The level of interaction is highly dependent upon the vertical effective stress at the time of permeation. At very low stress there may be an order of magnitude increase in GCL hydraulic conductivity (to about 6×10^{-11} m/s) as the permeant was changed from water to MSW leachate. At stress levels more typical of likely field conditions, the effect is far less significant with a hydraulic conductivity to MSW leachate still very low at 3×10^{-11} m/s.
- GCLs have the potential to provide strong attenuation of many metals and metalloids present in acid rock drainage (ARD) leachate and a neutral-pH gold mining leachate (GML). The hydraulic conductivity of the GCLs permeated with ARD increased from 2.8×10^{-12} m/s to 3.7×10^{-11} m/s after 35 pore volumes of permeation. There was no significant change in hydraulic conductivity for GCLs permeated with GML.
- There is negligible flow of hydrocarbons through a saturated GCL until a critical threshold pressure is exceeded. This threshold pressure is greater than that likely to be experienced in many applications and hence a hydrated GCL is likely to be an excellent barrier to hydrocarbons under these conditions. Above this threshold pressure the effect on intrinsic permeability is largely masked by the effect on density and viscosity such that the hydraulic conductivity of GCLs remains low and it appears that GCLs such as those tested can provide good containment of hydrocarbons for many practical applications.
- Up to 150 freeze-thaw cycles had very little effect on the hydraulic conductivity of GCLs permeated with water under conditions where there was no chemical interaction (cation exchange) with the bentonite prior to permeation. More research is required to assess the potential combined effect of cation exchange and freeze-thaw cycles at relatively low stress on the long-term performance of GCLs used in covers and similar near surface applications.
- 50 to 100 freeze-thaw cycles reduces the breakthrough pressure for permeation by jet fuel through a GCL. This was attributed to an increase in the size of macro pores in the bentonite following repeated freeze-thaw cycles. The hydraulic conductivity after up to 50 freeze-thaw cycles in the laboratory was less than 3×10^{-11} m/s at a gradient just above that required to initiate flow. There was some increase in hydraulic conductivity with 100 freeze-thaw cycles with a maximum value of about 1×10^{-10} m/s.
- The hydraulic conductivity (with respect to jet fuel) of GCL recovered from the field in the arctic after 3 years was less than 3×10^{-12} m/s at a pressure just above the breakthrough pressure. Increasing the gradient increases the hydraulic conductivity to 6×10^{-11} m/s. This higher value is at a gradient unlikely to be encountered in a real field situation but is still very low.
- Different GCLs have substantially different susceptibilities to internal erosion that can occur at high hydraulic gradients (e.g. in pond and lagoon applications). The choice of GCL carrier geotextile plays a key role in this different performance. GCLs with a woven geotextile in contact with the underlying subgrade did not perform as well as the other GCLs. GCLs with a nonwoven geotextile performed better than the GCLs with a woven over the subgrade but still experienced internal erosion over a geonet at high heads. In contrast, the scrim-reinforced GCL with a carrier geotextile mass of 350 g/m^2 did not exhibit any sign of internal erosion when placed over the geonet, gravel or sand tested at heads of 40-60 m.
- All the GCLs tested performed well with respect to internal erosion when on a suitable sand subgrade.

- The available evidence would suggest that temperatures of 30-40 °C can be expected at the top of the primary liner for MSW landfills. Higher temperatures (40-60 °C) can occur in situations where there is sufficient moisture to accelerate biodegradation of organic waste (*e.g.* in bioreactor landfills or when there is no operating leachate collection system) or due to hydration of incinerator ash.
- Diffusive and advective transport are, respectively, 100% and 80% higher at 35 °C than at a common groundwater temperature of 10 °C.
- The temperature of the GM in a secondary liner will be highly dependant on the nature of the primary liner. For a geocomposite primary liner comprised of only a GM and GCL, the secondary GM temperature may be expected to be only a few degrees (at most) less than that of the primary GM. As the thickness of the primary liner increases (*e.g.* if there is a foundation layer below the GCL as part of the primary liner or if there is a CCL), the temperature of the secondary GM decreases. The temperature of the primary and secondary GM may have a profound impact on the service life of these GMs.
- Both GCLs and CCLs may be susceptible to shrinkage and desiccation when used as part of a composite liner. This results from exposure to solar radiation prior to placement of adequate cover over the GM or after placement of waste (due to heat generated by the waste as discussed above). The potential for shrinkage and desiccation will depend on the temperature gradient, the characteristics of the GCL or CCL, the unsaturated soil characteristics and initial water content of the foundation layer beneath the clay liner, the overburden stress, and the distance to the underlying watertable. The available information suggests that while there is potential for desiccation and shrinkage, this can be mitigated by appropriate design and construction.
- Typical construction practice will result in GMs developing a significant number of wrinkles (waves) by the time they are covered. Techniques have been developed for quantifying the size and distribution of wrinkles.
- Under typical applied loads, wrinkles tend to remain in the GM. A gap typically remains between the GM wrinkle and a GCL. For a GM with wrinkles initially up to 60 mm high over a CCL, the gap may be filled at stress levels of 100 kPa or more when the CCL is compacted at the plastic limit. The lower the water content of the CCL at the time of compaction (relative to the plastic limit) the higher the pressure needed to extrude sufficient clay to fully close the gap.
- While needle-punched nonwoven geotextiles may provide reasonable protection against short-term holes in an underlying GM (*i.e.* limiting the number of holes to less than about 12 per hectare after placement of the drainage layer), recent research has shown that if gravel is used as the drainage layer (the preferred choice for providing good long-term leachate collection) then typical geotextile protection layers (up to 2000 g/m²) will not prevent large local strains in the GM and thinning of any underlying GCL (especially near wrinkles). Additional research is needed to clarify the time dependent effects of strains induced in GMs and the GCL by the gravel particles. Nevertheless it is clear that a sand protection layer between the gravel and the GM (perhaps combined with a traditional nonwoven geotextile) provides the best potential long-term performance.
- Field evidence of significant increases in leakage into LDS due to damage to composite liners involving a GM and GCL due to landfill activities after liner construction highlight the need to place an adequate protection layer above the composite liner to minimize the risk of such accidental damage. It also highlights the need to closely monitor not only the construction of the liner but also any waste placement or other work that could potentially cause damage to the liner.

- Field data indicates that the leakage through a GM/CCL composite liner was typically one to two orders of magnitude higher than that observed for GM/GCL composite liners.
- The calculated leakage obtained assuming direct contact (no major wrinkles) and typical size and number of holes in GMs using commonly used equations significantly underestimated the observed leakage for both GM/CCL and GM/GCL systems.
- The typical observed leakage for composite liners with CCLs and GCLs can be readily explained by holes in wrinkles for the typical number of holes/ha and reasonable combinations of other parameters using the Rowe (1998) equation.
- The design and construction of systems with a geonet leak detection system must ensure that the swelling and intrusion (under vertical stress) of any overlying GCL does not compromise the drainage function of the underlying geonet.
- Available field data suggests that even with typical numbers of wrinkles and holes per hectare, for landfills with good CQC/CQA and where there is no damage to the liner during landfilling activities, the post-closure leakages are very small and contaminant transport is likely to be controlled by diffusion through the liner system for contaminants that can readily diffuse through a GM.
- Volatile organic compounds (VOCs) can diffuse through both GMs and GCLs. Typical diffusion coefficients have been reported for both HDPE GMs as well as GCLs. Diffusion of hydrocarbons is much slower for fluorinated HDPE (f-HDPE) than conventional HDPE GMs. Control of the migration of these compounds will depend on the clay liner and any attenuation layer between the GM and any receptor aquifer.
- Ionic contaminants exhibit negligible diffusion through intact HDPE GMs. The diffusion coefficient for ionic contaminants through GCLs is a function of the bulk void ratio of the GCL.
- For landfills with double liner systems, the leakage through the primary liner will be mostly collected by the LDS. This will minimize the potential for advective movement through the secondary liner. However volatile organic compounds will volatilize in the leak detection system and can then diffuse through the underlying secondary composite liner, and hence diffusion needs to be considered for these cases. The time for VOCs to migrate through the primary liner at detectable levels can range from as little as a year to a decade depending on the thickness of the primary liner and the concentration in the landfill leachate collection system.
- The long-term performance of a GM will depend on the GM properties (*e.g.* its stress crack resistance, crystallinity, and oxidative induction), the tensile strains in the GM (which can be induced by the overlying drainage material and wrinkles in the GM), the exposure to chemicals in the leachate, and temperature.
- The service life of HDPE GMs meeting GRI GM-13 and used in MSW landfills are projected to be of the order of 600 years or more at a temperature less than 20 °C. At a temperature of 35 °C, the service life is projected to be of the order of 130-190 years. At temperatures of 50-60 °C, service lives are very short (15-50 years).
- Immersion of HDPE GMs in Jet A-1 accelerates antioxidant depletion relative to that observed in water or MSW leachate. The antioxidant depletion time was estimated to be about 2 and 6 years for untreated and fluorinated GMs, respectively, at 23 °C. This can be compared with a projected 20 years and 90 years based on GMs immersed in MSW leachate and water respectively (at 23 °C).

The evidence reviewed in this paper suggests that GCLs and GMs can play a very beneficial role in providing environmental protection. Like all engineering materials they must be used appropriately and consideration should be given to factors such as those addressed in this paper. There is a need for site specific design, strict adherence to construction specifications, and appropriate protection of the geosynthetics after construction. In particular, given the diversity of available GCLs and their different engineering characteristics, GCLs should be selected based on the required engineering properties, not just price.

12 – ACKNOWLEDGEMENTS

The author greatly appreciates the invitation of the Portuguese Geotechnical Society to present the 23rd Manuel Rocha Lecture. He is indebted to the many students and collaborators who have contributed to the research summarized in this paper. The assistance of the following graduate students in preparing figures is gratefully acknowledged: A. Hoor (Figs. 4 and 5), M. Chappel (Figs. 6 and 7), S. Dickinson (Figs 9 and 10), K. Abdel-Atty (Figs. 11-13) and M.Z. Islam (Fig 15). This work was funded by a variety of agencies including the Natural Sciences and Engineering Research Council of Canada (NSERC), the North Warning System Office of the Department of National Defense Canada, EarthTech (an Ontario Centre of Excellence), Terrafix Geosynthetics Inc., and NAUE GmbH & Co. The careful review by Dr. Ennio Palmeira and Dr. J-P Giroud, and the value of discussion with Dr. J-P Giroud, Mr. K. Von Mauberge and Mr. B. Herlin is gratefully acknowledged. The author is also very grateful to Ms. Sera Sheridan for her assistance in the preparation of this paper.

13 – REFERENCES

- Abollino, O.; Aceto, M.; Malandrino, M.; Sarzanini, C. & Mentasti, E. (2003) – Adsorption of HMs on Na-montmorillonite. *Water Res.*, v. 37, pp. 1619-1627.
- Ashmawy, A.; El-Hajji, D.; Sotelo, N. & Muhammad, N. (2002) – Hydraulic performance of untreated and polymer-treated bentonite in inorganic landfill leachates. *Clays Clay Miner.*, v. 50:5, pp. 545-551.
- August, H. & Tatzky, R. (1984) – Permeability of commercially available polymeric liners for hazardous landfill leachate organic constituents. *Proc. Int. Conf. on Geomembranes, IFAI, Denver*, v. I, pp. 163-168.
- August, H.; Tatzky-Gerth, R.; Preuschmann, R. & Jakob, I. (1992) – Permeationsverhalten von Kombinationsdichtungen bei Deponien und Altlasten Gegenueber Wassergefaehrdenden Stoffen. Project 10203412 of the BMBF, published by BAM, D-12200 Berlin, Germany.
- Badu-Tweneboah, K.; Giroud, J.P.; Carlson, D.S. & Schmertmann, G.R. (1998) – Evaluation of the effectiveness of HDPE geomembrane liner protection. *Proc. 6th International Conference on Geosynthetics, IFAI, Atlanta*, pp. 279-284.
- Basnett, C.R. & Bruner, R.J. (1993) – Clay desiccation of a single-composite liner system. *Geosynthetics 93, Vancouver, IFAI*, pp. 1329-1340.
- Bathurst, R.J.; Rowe, R.K.; Zeeb, B. & Reimer, K. (2006) – Ageocomposite barrier for hydrocarbon containment in the Arctic. *International Journal of Geoengineering Case Histories*, v. 1:1, pp. 18-34.

- Bonaparte, R.; Daniel, D. & Koerner, R.M. (2002) – Assessment and recommendations for improving the performance of waste containment systems. EPA Report, Co-operative Agreement Number CR-821448-01-0.
- Brain, E.S. (2000) – Evaluation of leachate compatibility to clay soil for three geosynthetic clay liner products. Geotechnical Special Publication, 103, GeoDenver 2000 Congress Advances in Transportation and Geoenvironmental Systems Using Geosynthetics, Denver, pp. 117-128.
- Brune, M.; Ramke, H.G.; Collins, H. & Hanert, H.H. (1991) – Incrustations process in drainage systems of sanitary landfills. Proc. 3rd Int. Landfill Symp., Cagliari, pp. 999-1035.
- Chappel, M.J.; Brachman R.W.I.; Take W.A. & Rowe R.K. (2007) – Development of a low altitude aerial photogrammetry technique to quantify geomembrane wrinkles. Geosynthetics 2007, Proc. Environmental Conference, Washington, pp. 293-300.
- Collins, H.J. (1993) – Impact of the temperature inside the landfill on the behaviour of barrier systems. Proc. 4th Int. Landfill Symp., Cagliari, v. 1, pp. 417-432.
- Colucci, P. & Lavagnolo, M.C. (1995) – Three years field experience in electrical control of synthetic landfill liners. Proc. 5th International Landfill Symposium, S. Margherita di Pula, pp. 437-452.
- Cooper, C.; Jiang, J.Q. & Ouki, S. (2002) – Preliminary evaluation of polymeric Fe & Al modified clays as adsorbents for heavy metal removal in water treatment. J. Chem. Tech. Biotechnol., v. 77, pp. 546-551.
- Corser, P.; Pellicer, J. & Cranston, M. (1992) – Observations on long-term performance of composite clay liners and covers. Geotech. Fabrics Report, Nov., pp. 6-16.
- Daniel, D.E.; Shan, H.Y. & Anderson, J.D. (1993) – Effects of partial wetting on the performance of the bentonite component of a geosynthetic clay liner. Proc. Geosynthetics 93, Industrial Fabrics Association International, St. Paul, Minn., v. 3, pp. 1483-1496.
- Dickinson, S. & Brachman R.W.I. (2006) – Deformations of a geosynthetic clay liner beneath a geomembrane wrinkle and coarse gravel. Geotextiles and Geomembranes, v. 24:5, pp. 285-298.
- Dobras, T.N. & Elzea, J.M. (1993) – *In-situ* soda ash treatment for contaminated Geosynthetic Clay Liners, Proc. Geosynthetics 93, Industrial Fabrics Association International, St. Paul, pp. 1145-1160.
- Egloffstein, T. (2001) – Natural bentonites -influence of the ion exchange and partial desiccation on permeability and self-healing capacity of bentonites used in GCLs. Geotextiles and Geomembranes, v. 19, pp. 427-444.
- Egloffstein, T. (2002) – Bentonite as sealing material in geosynthetic clay liners - Influence of the electrolytic concentration, the ion exchange and ion exchange with simultaneous partial desiccation on permeability. Zanzinger, H.; Koerner, R. & Gartung, E. (eds) Clay Geosynthetic Barriers. Swets and Zeitlinger, Lesse, pp. 141-153.
- Eloy-Giorni, C.; Pelte, T.; Pierson, P. & Margarita, R. (1996) – Water diffusion through geomembranes under hydraulic pressure. Geosynthetics Int., v. 3:6, pp. 741-769.
- Felon, R.; Wilson, P.E. & Janssens, J. (1992) – Résistance mécanique des membranes d'étanchéité. membranes armées en théorie et en pratique. In: Vade Mecum Pour la Réalisation des Systèmes d'Étanchéité Drainage Artificiels Pour les Sites d'Enfouissement Technique en Wallonie. Journées d'Études ULg 92.
- Giroud, J.P. (1997) – Equations for calculating the rate of liquid migration through composite liners due to geomembrane defects. Geosynthetics Int. v. 4:3-4, p. 335-348.

- Giroud, J.P. & Bonaparte, R. (1989) – Leakage through liners constructed with geomembranes - Part II. Composite liners. *Geotextiles and Geomembranes*, v. 8:2, pp. 71-111.
- Giroud, J.P. & Morel, N. (1992) – Analysis of geomembrane wrinkles. *Geotextile and Geomembranes*, v. 11:3, pp. 255-276 (Erratum: 1993, v. 12:4, pp. 378).
- Giroud, J-P & Soderman, K.L. (2000) – Criterion for acceptable bentonite loss from a GCL Incorporated into a liner system. *Gesynthetics International*, v. 7:4-6, pp. 529-581.
- Giroud, J.P. & Touze-Foltz, N. (2005) – Equations for calculating the rate of liquid flow through geomembrane defects of uniform width and finite or infinite length. *Geosynthetics International*, v. 12:4, pp. 191-204.
- Gudina, S. & Brachman, R.W.I. (2006a) – Physical response of geomembrane wrinkles overlying compacted clay. *Journal of Geotechnical and Geoenvironmental Engineering*, v. 132:10, pp. 1346-1353.
- Gudina, S. & Brachman, R.W.I. (2006b) – Effect of boundary conditions on deflection of GM wrinkles in a GM/GCL composite liner. *Proc. 8th International Geosynthetics Conference*, Yokohama, pp. 255-258.
- Guyonnet, D.; Gaucher, E.; Gaboriau, H.; Pons, C.; Clinard, C.; Norotte, V. & Didier, G. (2005) – Geosynthetic clay liner interaction with leachate: Correlation between permeability, microstructure, and surface chemistry. *Journal of Geotechnical and Geoenvironmental Engineering*, v. 131:6, pp. 740-749.
- Harpur, W.A.; Wilson-Fahmy, R.F. & Koerner, R.M. (1993) – Evaluation of the contact between geosynthetic clay liners and geomembranes in terms of transmissivity. *GRI Seminar on Geosynthetic Liner Systems*, Philadelphia, IFAI, pp. 143-154.
- Haxo Jr., H.E. & Lahey, T. (1988) – Transport of dissolved organics from dilute aqueous solutions through flexible membrane liner. *Haz. Waste & Hazardous Materials*, v. 5, pp. 275-294.
- Heibrock, G. (1997) – Desiccation cracking of mineral sealing liners. *Proc. 6th Int. Landfill Symp., Cagliari*, v. 3, pp. 101-113.
- Hewitt, R.D. & Daniel, D. E. (1997) – Hydraulic conductivity of geosynthetic clay liners after freeze-thaw. *Journal of Geotechnical and Geoenvironmental Engineering*, v. 123:4, pp. 305-313.
- Hsuan Y.G. & Koerner R.M. (1998) – Antioxidant depletion lifetime in high density polyethylene geomembranes. *J. Geotech. Geoenv. Eng.*, v. 124:6, pp. 532-541.
- Huang, C.H.; Wu, C.K. & Sun, P.C. (1999) – Removal of heavy metals from plating wastewater by crystallization/precipitation of gypsum. *J. Chin. Chem. Soc.*, v. 46:4, pp. 633-638.
- Islam, M.Z. & Rowe, R.K (2007) – Leachate composition and antioxidant depletion from HDPE geomembranes. *Geosynthetics 2007, Proc. Environmental Conference*, Washington, pp. 147-159.
- James, A.; Fullerton, D. & Drake, R. (1997) – Field performance of GCL under ion exchange conditions. *J. of Geotechnical and Geoenvironmental Engineering*, v. 123, pp. 897-901.
- Jo, H.; Katsumi, T.; Benson, C. & Edil, T. (2001) – Hydraulic conductivity and swelling of non-prehydrated GCLs permeated with single-species salt solutions. *J. of Geotechnical and Geoenvironmental Engineering*, v. 127, pp. 557-567.
- Jo, H.; Benson, C. & Edil, T. (2004) – Hydraulic conductivity and cation exchange in non-prehydrated and prehydrated bentonite permeated with weak inorganic salt solutions. *Clays and Clay Minerals*, v. 52:6, pp. 661-679.

- Jo, H.-Y.; Benson, C.H., Shackelford, C.D.; Lee, J.-M. & Edil, T.B. (2005) – Long-term hydraulic conductivity of a geosynthetic clay liner (GCL) permeated with inorganic salt solutions. *Journal of Geotechnical and Geoenvironmental Engineering*, v. 131:4, pp. 405-417.
- Jo, H.; Benson, C. & Edil, T. (2006) – Rate-limited cation exchange in thin bentonitic barrier layers. *Canadian Geotechnical J.*, v. 43, pp. 370-391.
- Katsumi, T. & Fukagawa, T. (2005) – Factors affecting the chemical compatibility and the barrier performance of GCLs. *Proc. 16th ICSMGE, Osaka*, pp. 2285-2288.
- Klein, R.; Baumann T.; Kahapka E. & Niessner R. (2001) – Temperature development in a modern municipal solid waste incineration (MSWI) bottom ash landfill with regard to sustainable waste management. *Journal of Hazardous Materials*, v: B83, pp. 265-280.
- Kodikara, J.K.; Rahman, F. & Barbour, S.L. (2002) – Towards a more rational approach to chemical compatibility testing of clay. *Canadian Geotechnical Journal*, v. 39, pp. 597-607.
- Koerner, G.R. & Koerner R.M. (2006) – Long-term temperature monitoring of geomembranes at dry and wet landfills. *Geotextiles and Geomembranes*, v. 24:1, pp. 72-77.
- Koerner, R.M.; Wilson-Fahmy, R.F. & Narejo, D. (1996) – Puncture protection of geomembranes. Part III: Examples. *Geosynthetics International*, v. 3:5, pp. 655-675.
- Kolstad, D.C.; Benson, C.H. & Edil, T.B. (2004) – Hydraulic conductivity and swell of nonprehydrated geosynthetic clay liners permeated with multispecies inorganic solutions. *Journal of Geotechnical and Geoenvironmental Engineering*, v. 130:12, pp. 1236-1249.
- Kraus, F.J.; Benson, H.C.; Erickson, E.A. & Chamberlain, J.E. (1997) – Freeze - Thaw cycling and hydraulic conductivity of bentonite barriers. *Journal of Geotechnical and Geoenvironmental Engineering*, v. 123:3, pp. 229-238.
- Lake, C.B. & Rowe, R.K. (2000) – Diffusion of sodium and chloride through geosynthetic clay liners. *Geotextiles and Geomembranes*, v. 18:2, pp. 102-132.
- Lake, C.B. & Rowe, R.K. (2004) – Volatile organic compound (VOC) diffusion and sorption coefficients for a needlepunched GCL. *Geosynthetics Int.*, v. 11:4, pp. 257-272.
- Lange, K.; Rowe, R.K. & Jamieson, H. (2004) – Metal migration in geosynthetic clay liners. *Proc. 57th Canadian Geotechnical Conference, Quebec City, Section 3D*, pp. 15-22.
- Lange, K.; Rowe, R.K. & Jamieson, H. (2005) – Attenuation of heavy metals by geosynthetic clay liners. *Proc. Geo-Frontiers Conference, Austin, Paper GRI-18, 8 p.*, CD-ROM.
- Lange, K.; Rowe, R.K. & Jamieson, H. (2007) – Metal retention in geosynthetic clay liners following permeation by different mining solutions. *Geosynthetics International*, (in review).
- Lee, J.-M. & Shackelford, C.D. (2005) – Impact of bentonite quality on hydraulic conductivity of geosynthetic clay liners. *Journal of Geotechnical and Geoenvironmental Engineering*, v. 131:1, pp. 64-77.
- Legge, K.R. & Davies, P.L. (2002) – An appraisal of the performance of geosynthetics material used in waste disposal facilities in South Africa. *WasteCon 2002, Durban, 12 p.*, CD-ROM.
- Li, L.Y. & Li, F. (2001) – Heavy metal sorption and hydraulic conductivity studies using three types of bentonite admixes. *Journal of Environmental Engineering*, v. 127, pp. 420-429.
- McKelvey, J.A. (1997) – *Geosynthetic Clay Liners in Alkaline Environments. Testing and Acceptance Criteria for GCLs*, ASTM STP 1308. Well, Larry W. (ed), ASTM, West Conshohocken, pp. 139-149.

- Melchior, S. (1997) – *In-situ* studies on the performance of landfill caps. Proc. International Containment Technology Conference, Florida State University, Tallahassee, pp. 365-373.
- Melchior, S. (2002) – Field studies and excavations of geosynthetic clay barriers in landfill covers. Zanzinger, H.; Koerner, R. & Gartung, E. (eds) Clay Geosynthetic Barriers. Swets and Zeitlinger, Lesse, pp. 321-330.
- Mazzieri, F. & Pasqualini, E. (2000) – Permeability of damaged geosynthetic clay liners. Geosynthetics International, v. 7:2, pp. 101-118.
- Mueller, W. & Jacob, I. (2003) – Oxidative resistance of HDPE. Polymer Degradation and Stability, v. 79, pp. 161-172.
- Müller, W.; Jakob, R.; Tatzky-Gerth, R. & August, H. (1998) – Solubilities, diffusion and partitioning coefficients of organic pollutants in HDPE geomembranes: Experimental results and calculations. Proc. 6th Int. Conf. on Geosynthetics, Atlanta, IFAI, pp. 239-248.
- Narejo, D.; Koerner, R.M. & Wilson-Fahmy, R.F. (1996) – Puncture protection of geomembranes Part II: Experimental. Geosynthetics International, v. 3:5, pp. 629-653.
- Nosko, V. & Touze-Foltz, N. (2000) – Geomembrane liner failure: Modeling of its influence on contaminant transfer. Proc. 2nd European Geosynthetics Conf., Bologna, p. 557-560.
- Olsen, H.W. (1961) – Hydraulic Flow Through Saturated Clays. D.Sc. Thesis, Massachusetts Institute of Technology, Cambridge.
- Osawa, Z. & Saito, T. (1978) – The effects of transition metal compounds on the thermal oxidative degradation of polypropylene in solution. In: Stabilisation and Degradation of Polymers, Advances in Chemistry, Series 169. Am. Chem. Soc., Washington, DC, pp. 2897-2907.
- Othman M.A.; Bonaparte, R. & Cross, B.A. (1996) – Preliminary results of study of composite liner field performance. Proc. 10th GRI Conf.: Field Performance of Geosynthetics and Geosynthetic Related Systems. Drexel University: Philadelphia, pp. 110-137.
- Pelte, T.; Pierson, P. & Gourc, J.P. (1994) – Thermal analysis of geomembranes exposed to solar radiation. Geosynthetics Int., v. 1:1, pp. 21-44.
- Petrov, R.J. & Rowe, R.K. (1997) – Geosynthetic clay liner compatibility by hydraulic conductivity testing: Factors impacting performance. Canadian Geotechnical Journal, v. 34:6, pp. 863-885.
- Petrov, R.J.; Rowe, R.K. & Quigley, R.M. (1997) – Selected factors influencing GCL hydraulic conductivity. Journal of Geotechnical and Geoenvironmental Engineering, v. 123:8, pp. 683-695.
- Podgorney R.K. & Bennett J.E. (2006) – Evaluating the long-term performance of geosynthetic clay liners exposed to freeze-thaw. J. Geotech. Geoenviron. Eng., v. 132:2, pp. 265-268.
- Reddy, K.R.; Bandi, S.R.; Rohr, J.J.; Finy, M. & Siebken, J. (1996) – Field evaluation of protective covers for landfill geomembrane liners under construction loading. Geosynthetics International, v. 3:6, pp. 679-700.
- Rowe, R.K. (1998) – Geosynthetics and the minimization of contaminant migration through barrier systems beneath solid waste. Keynote Lecture, Proc. Sixth International Conference on Geosynthetics, Atlanta, v. 1, pp. 27-103, Industrial Fabrics Association International, St. Paul. (This paper can be downloaded from www.geoeng.ca).
- Rowe, R.K. (2005) – Long-term performance of contaminant barrier systems. 45th Rankine Lecture. Geotechnique, v. 55:9, pp. 631-678.

- Rowe, R.K. (2006) – Some factors affecting geosynthetics used for geoenvironmental applications. Keynote Lecture, 5th International Conference on Environmental Geotechnics, Cardiff, v. 1, pp. 43-69.
- Rowe, R.K. & Orsini, C. (2003) – Effect of GCL and subgrade type on internal erosion in GCLs. *Geotextiles and Geomembrane*, 21:1, pp. 1-24.
- Rowe, R.K. & Hoor, A. (2007) – Temperature of secondary liners in municipal solid waste landfills. *Geosynthetics 2007, Proc. Environmental Conference*, Washington, pp. 132-146.
- Rowe, R.K. & Rimal, S. (2007) – Depletion of antioxidant from HDPE geomembrane in a composite liner. *Journal of Geotechnical and Geoenvironmental Engineering* (in press).
- Rowe, R.K.; Mukunoki, T.; Li, H.M. & Bathurst R.J. (2004a) – Effect of freeze-thaw on the permeation of arctic diesel through a GCL. *Journal of ASTM International*, v: 1:2, pp. 134-146. Available online: www.astm.org; 1 February 2004, 10 p. This was also published by ASTM in hardcopy in *Advances in: Geosynthetic Clay Liner Technology* R.E. Mackey & von Maubeuge, K. (eds).
- Rowe, R.K.; Quigley, R.M.; Brachman, R.W.I. & Booker, J.R. (2004b) – *Barrier Systems for Waste Disposal Facilities*. Taylor & Francis Books Ltd (E & FN Spon), London, 587 p.
- Rowe, R.K.; Hurst, P. & Mukunoki, T. (2005a) – Permeating partially hydrated GCLs with jet fuel at temperatures from -20 °C and 20 °C. *Geosynthetics International*, 12:6, pp. 333-343.
- Rowe, R.K.; Mukunoki, T. & Sangam, P.H. (2005b) – BTEX diffusion and sorption for a geosynthetic clay liner at two temperatures. *Journal of Geotechnical and Geoenvironmental Engineering*, v. 131:10, pp. 1211-1221.
- Rowe, R.K.; Mukunoki, T.; Bathurst, R.J.; Rimal, S.; Hurst, P. & Hansen, S. (2005c) – The performance of a composite liner for retaining hydrocarbons under extreme environmental conditions. *Geofrontiers 2005*, Austin, 17 p, CD-Rom.
- Rowe, R.K.; Mukunoki, T. & Bathurst, R.J. (2006) – Compatibility with Jet A-1 of a GCL subjected to freeze-thaw cycles. *Journal of Geotechnical and Geoenvironmental Engineering*, v. 132:12, pp. 1519-1643.
- Rowe, R.K.; Mukunoki, T. & Bathurst, R.J. (2007a) – Hydraulic conductivity to Jet-A1 of GCLs subjected to up to 100 freeze-thaw cycles. *Geoengineering Centre at Queen's-RMC Research report*.
- Rowe, R.K.; Mukunoki, T.; Bathurst, R.J.; Rimal, S.; Hurst, P. & Hansen, S. (2007b) – Performance of a geocomposite liner for containing Jet A-1 spill in an extreme environment. *Geotextiles and Geomembranes* (in press).
- Rowe, R.K.; Sangam, H.P. & Lake, C.B. (2003) – Evaluation of an HDPE geomembrane after 14 years as a leachate lagoon liner. *Canadian Geotechnical Journal*, v. 40:3, pp. 536-550.
- Ruhl, J.L. & Daniel, D.E. (1997) – Geosynthetic clay liners permeated with chemical solutions and leachates. *Journal of Geotechnical and Geoenvironmental Engineering*, v. 123:4, pp. 369-380.
- Sangam, H.P. & Rowe, R.K. (2001) – Migration of dilute aqueous organic pollutants through HDPE geomembranes. *Geotextiles and Geomembranes*, v. 19:6, pp. 329-357.
- Sangam, H.P. & Rowe, R.K. (2002) – Effects of exposure conditions on the depletion of antioxidants from high density polyethylene (HDPE) geomembranes. *Canadian Geotechnical Journal*, v. 39:6, p. 1221-1230.

- Sangam, H.P. & Rowe, R.K. (2005) Effect of surface fluorination on diffusion through an HDPE geomembrane. *Journal of Geotechnical and Geoenvironmental Engineering*, v. 131:6, p. 694-704.
- Schubert, W.R. (1987) – Bentonite matting in composite lining systems. *Geotechnical Practice for Waste Disposal 87*, Woods, R.D. (ed), ASCE, New York, p. 784-796.
- Shackelford, C.D. (2005) – Environmental issues in geotechnical engineering. *Proc. 16th International Conference on Soil Mechanics and Geotechnical Engineering*, Osaka, p. 12-16, Millpress, Rotterdam, v. 1, p. 95-122.
- Shackelford, C.; Benson, C.; Katsumi, T. & Edil, T. (2000) – Evaluating the hydraulic conductivity of GCLs permeated with non-standard liquids. *Geotextiles and Geomembranes*, v: 18:2-3, pp. 133-161.
- Shan, H.Y. & Daniel, D.E. (1991) – Results of laboratory tests on a geotextile/ bentonite liner material. *Proc. Geosynthetics 91*, Industrial Fabrics Association International, St. Paul, v. 2, pp. 517-535.
- Shan, H. & Lai, Y. (2002) – Effect of hydrating liquid on the hydraulic properties of geosynthetic clay liners. *Geotextile and Geomembranes*, v. 20, pp. 19-38.
- Shaner, K.R. & Menoff, S.D. (1992) – Impacts of bentonite geocomposites on geonet drainage. *Geotextiles and Geomembranes*, v: 11:4-6, pp. 503-512.
- Soong, T.Y. & Koerner, R.M. (1998) – Laboratory study of high density polyethylene geomembrane waves. *Proc. 6th Int. Conf. on Geosynthetics*, Atlanta, IFAI, pp. 301-306.
- Southen, J.M. (2005) – Thermally Driven Moisture Movement Within and Beneath Geosynthetic Clay Liner. PhD Thesis, University of Western Ontario, 320 p.
- Southen, J.M. & Rowe, R.K. (2004) – Investigation of the behavior of geosynthetic clay liners subjected to thermal gradients in basal liner applications. *J. of ASTM International*, v. 1:2 ID JAI11470, Available online: www.astm.org; 13 p. Also ASTM: *Advances in Geosynthetic Clay Liner Technology*. Mackey, R.E. & von Maubeuge, K. (eds), p. 121-133.
- Southen, J.M. & Rowe, R.K. (2005) – Laboratory investigation of GCL desiccation in a composite liner subjected to thermal gradients. *J. Geotech. Geoenv. Eng.*, v. 131:7, pp. 925-935.
- Stam, T.G. (2000) Geosynthetic clay liner field performance. *Proc. 14th GRI Conference*, Las Vegas, pp. 242-254.
- Stichbury, M.K.; Bain, J.G.; Blowes, D.W. & Gould, W.D. (2000) – Microbially mediated reductive dissolution of arsenic-bearing minerals in a gold mine tailings impoundment. *ICARD 2000, Proc. 5th International Conf. on Acid Rock Drainage*, v. 1, pp. 97-106.
- Stone, J.L. (1984) – Leakage monitoring of the geomembrane for proton decay experiment. *Int. Conf. on Geomembranes*, Denver, v. 2, pp. 475-480.
- Thiel, R. & Richardson, G.N. (2005) – Concern for GCL Shrinkage when installed on slopes. *ASCE Geo-Frontiers C*, Austin, Paper GRI-18, 7 p., CD-ROM.
- Thiel, R. & Smith, M.E. (2004) – State of the practice review of heap leach pad design issues. *Geotextiles and Geomembranes*, v. 22:6, pp. 555-568.
- Thiel, R.; Giroud, J.P.; Erickson, R.; Criley, K. & Bryk, J. (2006) – Laboratory measurements of GCL shrinkage under cyclic changes in temperature and hydration conditions. *Proc. 8th International Geosynthetic Conference*, Yokohama, pp. 157-162.

- Tognon, A.R.; Rowe, R.K.&Moore, I.D. (2000) – Geomembrane strain observed in large-scale testing of protection layers. *J. Geotech. Geoenv. Eng.*, v. 126:12, pp. 1194-1208.
- Touze-Foltz, N. & Giroud, J.P. (2005) – Empirical equations for calculating the rate of liquid flow through composite liners due to large circular defects in the geomembrane. *Geosynthetics International*, v. 12:4, pp. 205-207.
- Touze-Foltz, N.; Schmittbuhl, J. & Memier, M. (2001) – Geometric and spatial parameters of geomembrane wrinkles on large scale model tests. *Geosynthetics 2001*, Portland, pp. 715-728.
- Viebke, J.; Elble, E.; Ifwarson, M. & Gedde, U.W. (1994) – Degradation of unstabilized medium-density polyethylene pipes in hot-water applications. *Polymer Eng. and Science*, v. 34:17, pp. 1354-1361.
- Wilson-Fahmy, R.F.; Narejo, D. & Koerner, R.M. (1996) – Puncture protection of geomembranes Part I: Theory. *Geosynthetics International*, v. 3:5, pp. 605-628.
- Workman J.P. (1993) – Interpretation of leakage rates in double lined systems. *Proc. 7th GRI Conf.: Geosynthetic Liner Systems*. Drexel University, Philadelphia, pp. 91-108.
- Wisse, J.D.M.; Broos, C.J.M.&Boels, W.H. (1990) – Evaluation of the life expectancy of polypropylene geotextiles used in bottom protection structures around the Ooster Schelde storm surge barrier: A case study. *Proc. 2nd Int. Conf. on Geotextiles*, Las Vegas, v. 1, pp. 283-288.
- Yong, R.N. (2001) – *Geo-environmental Engineering*, 1st ed, CRC Press LLC, 320 p.
- Yoshida, H. & Rowe, R.K. (2003) – Consideration of landfill liner temperature. *Proc. 9th. Int. Landfill Sym.*, Cagliari, Italy, CD-ROM.